HHS Public Access

Author manuscript

Nat Ment Health. Author manuscript; available in PMC 2025 August 01.

Published in final edited form as:

Nat Ment Health. 2024 August ; 2(8): 935–950. doi:10.1038/s44220-024-00266-6.

Stress-Resilience Impacts Psychological Wellbeing: Evidence from Brain-Gut Microbiome Interactions

Eric An[3,5,#], **Desiree R. Delgadillo**[1,2,3,4,5,#], **Jennifer Yang**[1,2,3,5], **Rishabh Agarwal**[1,5], **Jennifer S. Labus**[1,2,3,4,5], **Shrey Pawar**[1,5], **Madeline Lietman**[1,5], **Lisa A. Kilpatrick**[1,2,3,5], **Ravi R. Bhatt**[6], **Priten Vora**[1,2,3,5], **Allison Vaughan**[1,2,3,5], **Tien S. Dong**[1,2,3,4,5,*], **Arpana Gupta**[1,2,3,4,5,*]

[1]G. Oppenheimer Center for Neurobiology of Stress & Resilience, at UCLA

[2]UCLA Vatche and Tamar Manoukian Division of Digestive Diseases

[3]David Geffen School of Medicine at UCLA

[4]UCLA Goodman Luskin Microbiome Center

[5]University of California, Los Angeles

[6]Mark and Mary Stevens Neuroimaging and Informatics Institute, University of Southern California

Abstract

The brain-gut-microbiome (BGM) system plays an influential role on mental health. We characterized BGM patterns related to resilience using fecal samples and multimodal MRI. Data integration analysis using latent components showed the high resilience phenotype was associated with lower depression and anxiety symptoms, higher frequency of bacterial transcriptomes (related to environmental adaptation, genetic propagation, energy metabolism, anti-inflammation),

[*]**Corresponding authors:** Arpana Gupta, Ph.D., Associate Professor, Co-Director: Goodman Luskin Microbiome Center, G. Oppenheimer Center for Neurobiology of Stress and Resilience, Director: Neuroimaging Core; Ingestive Behavior and Obesity Program, UCLA Vatche and Tamar Manoukian Division of Digestive Diseases, David Geffen School of Medicine, UCLA CHS 42-210, 10833 Le Conte Avenue | Los Angeles, CA 90095-7378, AGupta@mednet.ucla.edu; Tien S. Dong, MD, PhD, Assistant Professor, G. Oppenheimer Center for Neurobiology of Stress and Resilience, Goodman Luskin Microbiome Center, Director: Biorepository Core; Liver Disease, UCLA Vatche and Tamar Manoukian Division of Digestive Diseases, David Geffen School of Medicine, UCLA CHS 42-210, 10833 Le Conte Avenue | Los Angeles, CA 90095-7378, TSDong@mednet.ucla.edu.

[#]Shared First Authorship

[*]Shared Senior Authorship

Author Contributions Statement:

EA, DRD: statistical analysis, drafting of the manuscript, critical revision of the manuscript for important intellectual content.

JY, RA, SP, ML, PV: statistical analysis, data interpretation, and visualization

JSL: data interpretation

AV: data collection

LAK, RRB: data interpretation, critical revision of the manuscript for important intellectual content

AG, TSD: funding, study concept and design, statistical analysis and interpretation of data, critical revision of the manuscript for important intellectual content, technical support, study supervision.

Competing Interests Statement: AG is scientific advisor to Yamaha.

All other authors have nothing to disclose.

Code Availability: Not relevant as all data analyses used readily available programs (e.g., and open sourced R code

Inclusion and Ethics Statement:

All procedures complied with institutional guidelines and were approved by the Institutional Review Board at UCLA's Office of Protection for Research Subjects. All participants provided written informed consent.

increased metabolites (N-acetylglutamate; dimethylglycine), and cortical signatures (increased resting state functional connectivity between reward circuits and sensorimotor networks; decreased grey matter volume and white matter tracts within the emotion regulation network). Our findings support a multi-omic signature involving the BGM system suggesting that resilience impacts psychological symptoms, emotion regulation and cognitive function as reflected by unique neural correlates and microbiome function supporting eubiosis and gut barrier integrity. Bacterial transcriptomes provided the highest classification accuracy suggesting that the microbiome is critical in shaping resilience and highlights that microbiome modifications can optimize mental health.

Introduction

Upwards of $300 billion dollars is lost annually due to stress-related health care costs and missed work in the U.S.[1] highlighting the need for greater resilience to stress. Definitions of resilience generally refer to beneficial outcomes in response to threat or stressful events[2,3]. Resilience involves positive acceptance of change, tolerance of negative affect, tenacity, and the ability to recover after stressful events[4]. Resilience can predict stress-related depression and anxiety[5,6], traumatic stress[7], and maladaptive coping mechanisms such as alcohol misuse[8]. Most research investigating resilience has focused its correlations with personality traits[9], emotional[10] and behavioral[11] regulation strategies, and social factors including supportive interpersonal relationships[12]. Resilience is also related to autonomic flexibility[13] and adaptive neurological correlates[11,14].

The composition and function of the human microbiome, an ecosystem consisting of trillions of microorganisms residing in and on the human body[15], have been linked to stress-related disorders and other mental health diagnoses[16–21]. The gut microbiome modulates psychological functioning by influencing the brain-gut microbiome (BGM) system[22], a bidirectional signaling mechanism between the central nervous system (CNS) and gastrointestinal tract[23]. Interestingly, the microbiome has been implicated in conferring stress-resilience[24,25]. Evidence reveals that alterations in BGM signatures can influence prosocial behaviors[26] related to resilience and stress-related psychopathologies[16–20]. Numerous animal studies also reveal the role of the BGM in resilience versus susceptibility traits after stress exposure. For example, gut microbial composition differed in mice susceptible compared to mice resilient to chronic social defeat stress[27,28], as well as to learned helplessness after exposure to inescapable stress[29,30]. This opens the intriguing possibility that the endogenous gut microbiome may house stress mitigating therapeutic metabolites supporting neurologically adaptive processes. For instance, bacterial transcriptomes are related to a number of microbiome functions[31] and serve to maintain a balanced and diverse population of gut microbiota (eubiosis) and gut barrier integrity. Thus, a resilient phenotype involves expression of transcriptomes that ensure appropriate modulation of the BGM system, and therefore, an adaptive CNS[24].

Collectively, the gut microbiota produces a number of metabolites, including hormones, neurotransmitters (such as Gamma-Aminobutyric Acid; GABA[32], glutamate[33], and serotonin[34]), and other signaling molecules within the BGM[35] implicated in stress-related

psychopathology[36,37]. Via serotonin, gut microbiota through neural activation of vagal afferents in the gut[38], can contribute to a regulated autonomic nervous system and adaptive stress response. The main metabolites produced by gut microbiota are short-chain fatty acids (SCFAs)[39] which are known to influence cognitive and emotional processing through effects on the brain via anti-inflammatory properties[40]. In animal studies, low SCFA has been associated with anxiety and depression-related behaviors[41] and also predicted resilience versus susceptibility to traumatic stress[42].

The gut microbiota can also shape brain structure and function[43–45], as evidenced by probiotic studies. Probiotics have resulted in decreased activity in somatosensory and viscerosensory cortices in response to emotional attentional tasks and reduced grey matter volume and increased resting state functional connectivity (rsFC) within the default mode network (DMN)[46]. A recent neuroscience review of resilience highlighted the mesolimbic reward system, the DMN, and regions involved in fear and stress, namely, the amygdala[47]. The DMN, activated during passive rest, daydreaming, and thinking about the past or others[48] has been linked to major depressive disorder (i.e., excessive rumination[49] but also dispositional mindfulness[50]). Resilience-related grey matter volume changes have been observed in cognitive and affective regions (amygdala, subgenual and rostral anterior cingulate cortex)[51,52]. Lower activity within the salience network[53] but increased connectivity within the sensorimotor network[54,55] and greater responses in reward circuits (basal ganglia)[56] have been linked to resilience. There are also associations between resilience and white matter tract integrity within structures implicated in social cognition[57].

Since no study to date has investigated an integrative biological profile of resilience, we aimed to determine how resilience is related to clinical phenomes, microbiome function, and neural characteristics (Figure 1). Considering the microbiome's role in influencing psychological resilience, we hypothesized that high resilience would be associated with: (1) lower scores on clinical measures of psychological symptoms and higher levels of adaptive coping; (2) microbiome function supporting gut health as evidenced by characteristic bacterial transcriptomes (pathways supporting gut microbial growth and diversity) and metabolome (metabolites supporting anti-inflammation and gut barrier integrity); (3) brain morphometry and connectivity signatures, reflecting increased efficiency in regions important for emotion regulation and cognitive functioning.

Results

Demographics and clinical results

Comparisons of clinical variables between the high resilience group (HR) and low resilience group (LR) are depicted in Table 1. The distribution of BMI that justifies the threshold for resilience group labels is illustrated in Supplementary Figure S1.

Microbiome analysis on group differences

The alpha and beta diversity did not show significant differences between HR and LR (Supplementary Figure S2 and S3). Performance of on the 16S-identified amplicon sequence

variants (ASVs) dataset was not found to be a significant contributor in the DIABLO model (AUC=0.524).

DIABLO identifies a multi-omic signature able to classify high and low resilience

DIABLO Model Performance.—DIABLO identified a highly correlated 'omics signature capable of discriminating between individuals with high versus low psychological resilience. A receiver operating characteristic (ROC) curve showing the performance of the classification model at all classification thresholds had an area under the ROC Curve (AUC; overall model) of 0.77 and the BER was 0.18. The training set AUC was 68% and the achieved overall testing set (N = 81) AUC was 68%. The training set (N=35) BER was 0.18. Area under the curve by dataset type was 77% for clinical, 63% for metabolome, 77% for transcriptome, 65% for structural MRI, 66% for resting-state functional MRI, and 48% for diffusion MRI. A summary of the final model's performance is in Supplementary Figure S4.

DIABLO-selected variables.—The standardized values of omics variables selected by the DIABLO model are depicted by resilience group in Figure 2. A total of 45 features, 13 clinical features, including survey sub-scores, 3 metabolome, 16 transcriptome, 6 structural MRI, 5 resting-state functional MRI, and 2 diffusion MRI variables were included in the final model and depicted in the loading plots of Figure 3. Variables from each dataset type are listed below in order of importance based on their loading vectors, which represent the magnitude of contribution to the DIABLO model. Higher loading vectors suggest greater importance in predicting resilience.

Clinical variables in order of importance included IPIP Neuroticism, STAI Anxiety, HAD Anxiety, FFM Total Score and the Describing FFM subscale, MASQ Verbal Memory, PSS Score, IPIP Extraversion, MASQ language, HAD Depression, FFM Non-judgement subscale, MASQ Visual Perception and Attention subscores. HR had higher mean levels of extraversion[58] and mindfulness[59] than their LR counterparts. Further, HR had lower mean levels of anxiety (HADS; STAI)[60,61], neuroticism[58], perceived stress, and difficulties with verbal memory, visual perception, language, and attention[62] than LR.

Metabolome variables in order of importance included N-acetylglutamate (NAG), dimethylglycine, and creatine. HR had higher mean levels of NAG and dimethylglycine, and similar mean levels of creatine compared to LR. Bacterial transcriptomes in order of importance are depicted in Figure 3 and their functions are listed in Figure 1E. In brief, mean levels of transcriptomes linked to environmental adaptation, genetic propagation, metabolism, and anti-inflammation (i.e., increased frequency of a transcriptome involved in SCFA production) were higher in HR compared to LR.

Structural MRI features in order of importance included right subcallosal gyrus (SbCaG) volume, SbCaG surface area (SA), left angular gyrus (AngG) volume, AngG SA, right inferior part of the precentral sulcus (InfPrCS) SA, and InfPrCS volume. The resting-state functional MRI features in order of importance included connectivity between the ventral tegmental area (VTA) and right thalamus, between the left mesencephalic reticular formation (MRF) and the right supramarginal gyrus(SuMarG), between the right inferior segment of the circular sulcus of the Insula (InfCirIns) and the left pallidum, between the

right subcentral gyrus and sulci (SbCG_S) and the left superior parietal lobule (SupPL), and between the right lateral orbital sulcus (LORs) and the left putamen. Diffusion MRI features in order of importance included connections between the right and left SbCaG, and between the right lateral orbital gyrus (SupOcG) and right hippocampus. HR had lower mean levels of all DIABLO-selected structural MRI features but higher mean levels of all resting-state functional MRI features than LR. Regarding diffusion MRI features, HR had lower mean levels in bilateral SbCaG connections but higher connections between the right SupOcG and right hippocampus.

There were also associations between different classes of DIABLO-selected omics variables that were unique to HR. For example, anxiety (HADS) was negatively associated with a transcriptome involved in SCFA production. Although there were positive associations between NAG and transcriptomes involved in anti-inflammatory response and environmental adaptation in both HR and LR, only HR had an additional positive association between NAG and a transcriptome involved in genetic propagation.

The entire model is depicted in the connectogram (Figure 4), where mean levels for each feature are visualized by resilience group in the data blocks forming the circle, and correlations between datasets are depicted inside the circle. Connectograms are built on a similarity matrix[63] and represent the correlation between variables from different datasets. A cutoff was chosen as $r > 0.55$ as this is universally considered a “moderate” correlation.

Spearman correlations.

Spearman correlations revealed two CD-RISC factors most robustly associated with DIABLO selected variables: control (sense of control and purpose in life, knowledge of where to turn for help) and persistence (personal competence, high standards, and tenacity; see Table 2). Additionally, Spearman’s rank correlations were performed to assess relations between all ASV’s on the genus level and DIABLO selected metabolites. Results showed that NAG was negatively associated with the genus Bacteroides rs (114) =−0.32, p=.004, q=.02.

Discussion

Our study shows that several key BGM markers distinguish HR from LR. HR exhibits adaptive psychological features, microbiome function facilitating gut health, and neurological signatures supporting emotion regulation and cognitive-emotional connections. Notably, among all data blocks, bacterial transcriptomes most strongly differentiated high from low resilience phenotypes. Furthermore, our findings suggest resilient individuals, particularly those demonstrating tenacity and perceived ability to control life outcomes, possess a microbiome that supports gut barrier integrity and eubiosis and a cortical signature that reflects adaptive emotional and cognitive regulation.

Association of resilience with clinical symptoms

In addition to higher levels of extraversion, HR was associated with lower scores of depression, anxiety, perceived stress, and neuroticism, which is consistent with previous literature[5,6,9,64,]. HR was also higher in trait-like mindfulness, particularly in abilities

to express emotions in words, be non-judgmental, and express empathy, which are characteristics linked to increased resilience to stress[65]. Additionally, HR was related to better self-reported cognitive abilities including verbal fluency, verbal memory, comprehension, visual memory, and sustained attention. Such cognitive skills have been associated with coping ability[11,66,67]. Collectively, these findings suggest low resilience individuals may deplete psychological and cognitive resources when confronted with stressful events while resilient individuals may instead reappraise stressful events to promote advantageous psychological outcomes and coping.

Association of resilience with gut transcriptomics and metabolites

The functional categories of transcriptomes associated with HR included adaptive response to environmental changes, genetic propagation, energy metabolism, and anti-inflammatory response. HR exhibited increased frequency of pathways that improve gut bacteria adaptation in unfavorable conditions (e.g., uptake of essential nutrients or extrusion of toxic substances; adjustment to fluctuations in pH and osmotic changes; communication within cellular community to adjust gene expression accordingly and cooperatively behave in virulence regulation, resource utilization, or even antibiotic resistance[68]). In support of bacterial adaptation, HR also exhibited increased frequency of pathways facilitating genetic proliferation and pathways providing bacterial energy sources (e.g., carbohydrate metabolism). In addition, HR exhibited increased frequency of pathways related to anti-inflammatory response; therefore, maintaining gut barrier integrity (e.g., metabolic degradation of lysine into SCFAs such as acetate and butyrate[40]). See Supplemental Table S1 for other transcriptomes associated with high resilience. Our findings were consistent with animal studies showing that high resilience phenotypes are associated with increased frequency of pathways related to SCFA production[41,42], as well as carbohydrate metabolism and genetic information processing[42]. Overall, HR possessed a microbiome that functions to maintain eubiosis and gut barrier integrity, thereby promoting intact communication between the gut and brain to optimize psychological functioning.

In the metabolome, HR was associated with higher levels of N-acetylglutamate (NAG) and dimethylglycine (DMG). Bacteria use NAG, derived from the amino acid glutamate, to synthesize arginine[69]. NAG's role in the BGM system is unclear. Increased levels of NAG may be secondary to endogenous metabolism or altered dietary intake, at least in healthy individuals[70]. In the present study, increased levels of NAG in HR were associated with higher frequency of metabolic pathways related to environmental adaptation and anti-inflammation. Increased levels of NAG may be associated with HR secondary to stimulating arginine synthesis which has anti-inflammatory effects in the gut[71]. On the other hand, DMG is derived from dietary amino acid glycine and is used in methylation reactions crucial for various metabolic pathways, including energy metabolism, anti-oxidative activity, and DNA synthesis and metabolism[72]. DMG has also been shown to increase gut microbiota strains involved in anti-inflammatory response (e.g., SCFA production)[73]. See Supplemental Table S1 for other metabolites associated with HR. Our findings show the HR group may host a gut microbiome that can withstand perturbations as evidenced by an increase in metabolites that quell inflammation which, in turn, may support optimal neurological processes.

Association of resilience with multimodal brain signatures

Regarding brain morphometry, HR was associated with reduced SbCG grey matter volume and surface area. The SbCG, an important node in a network including the limbic system and thalamus, is strongly associated with cognitive-emotional processing[74] and inhibiting fear responses[75]. Similarly, reduced anterior cingulate cortex volume (subcomponents of which include the SbCG) was associated with PTSD remission after treatment completion, showing that volume reduction may indicate neuroplastic changes evidencing increased emotional regulation and extinction of maladaptive cognitive-emotional connections[52]. Reduced SbCG volume was also positively associated with greater resilience subscale scores[51]. These morphological signatures suggest dampened but adaptive reactivity towards acute emotional challenges and greater brain efficiency[76], highlighting that resilient individuals may require less cognitive effort in emotion and fear modulation[11,76]. Gut microbiota alterations can also influence grey matter changes[44,77]. Taken together, a resilient individual demonstrates microbiome functions that exert characteristic CNS changes, which then provide the physiological means for adaptive coping.

HR was associated with decreased anatomical connectivity involving the right and left SbCG, regions linked to dysphoric mood[78]. Decreased anatomical connectivity between the bilateral SbCG regions may imply less activation of distressing emotions[79]. In addition, HR was associated with decreased anatomical connectivity involving the hippocampus, a region together with the amygdala that is involved in fear[80] and anxiety[79]. Based on these findings, HR demonstrates a stress-resilient neurological signature.

Several functional connections were significant in differentiating HR vs LR, including the reward circuit (e.g., basal ganglia), sensorimotor network (SMN), DMN, and brainstem. HR had increased rsFC between the reward circuit (ventral tegmental area, pallidum) and SMN (thalamus, insula). Connections between these regions are related to fear-related motor neurocircuitry and thought to be involved in maladaptive fear emotions[81,82]. Abnormal connectivity between these areas may be a vulnerability factor. For example, restricted range of emotion is a common symptom in stress-related mental health conditions like PTSD and depression[83], which highlights a possible link to reward circuitry alterations. Other brain networks associated with HR involved the DMN (supramarginal gyrus) and brainstem (MRF). Normal connectivity between the DMN and MRF may be a resilient characteristic given that self-monitoring (DMN) of threatening stimuli (MRF) facilitates readiness to react to stressors appropriately. The DMN may also play a role in resilience given its involvement in treatment recovery and “bouncing back” from trauma[55,84,85,]. DMN connectivity has also been linked to an abundance of certain gut microbiota[45]; therefore, it is plausible the microbiome optimizes stress response by modulating relevant areas of brain connectivity. Our findings highlight that a resilient individual demonstrates an intact BGM system that shapes connectivity within the CNS to allow for adaptive coping.

Association of resilience with integrated brain-gut interactions

Although SCFAs were nonsignificant predictors of resilience within our DIABLO model, lower anxiety scores in HR were associated with higher frequency of a transcriptome involved in SCFA production. Thus, an individual’s level of resilience may modulate

microbiome function to produce SCFAs and consequently mitigate stress-related conditions such as anxiety. Importantly, SCFAs are involved in maintaining intestinal barrier integrity[86] and anti-inflammation[87]. Lower anxiety scores in HR were also associated with a lower degree of neuroticism and perceived stress in life. In addition, increased frequency of certain bacterial transcriptomes in HR was associated with increased production of the bacterial metabolite, NAG. Such transcriptomic pathways may facilitate overall gut health by supporting increased production of NAG, a metabolite implicated in having anti-inflammatory effects in the gut. Furthermore, resilient individuals may be able to mitigate development of stress-related psychopathology due to bacterial transcriptomes aiding in maintaining overall gut health[69,88].

Conclusion and Clinical Implications

This study is the first to identify a HR BGM phenotype and reveals promising pathways by which the onset and severity of stress-related psychiatric conditions might be prevented or mitigated. This cross-sectional study provides theoretical support for the development of longitudinal studies needed to establish causality. While the current study focuses on healthy samples to facilitate identification of potential factors that enhance and maintain health, future studies should consider comparing microbial profiles of healthy controls to those presenting with psychiatric diagnoses such as depression or PTSD. Future work should also consider metabolomics analysis of plasma samples and, importantly, vagal tone as it may mediate the relation between stress-resistance and microbial composition. Interestingly, the afferent vagus nerve can differentiate between pathogenic and non-pathogenic bacteria and can transmit signals that either exacerbate or mitigate stress responses depending on the bacterial stimulus[89] making it a promising avenue for future inquiry. Some clinical implications to explore are whether dietary modifications, prebiotics, probiotics, or other clinical interventions (e.g., fecal transplantation) may improve coping and resilience to stress. Collectively, our findings support numerous avenues for novel inquiries and suggest that features of the brain and the gut microbiome work together to build stress-resilience.

Methods and Materials

Participants

A cohort of 116 healthy individuals (71 females) were recruited from the Los Angeles community through advertisements. Premenopausal women were included as determined by self-report of the last day of the previous menstrual cycle, and enrolled women were scanned during the follicular phase of the menstrual cycle. Participants were excluded if they had any major medical/neurological conditions, current or past psychiatric illnesses, gastroenterological issues, abdominal surgeries, substance use, tobacco dependence (half a pack or more daily), or metal implants (due to MRI contraindications); regularly used medications that interfere with the CNS; regularly used analgesics; were pregnant or breastfeeding; performed extreme strenuous exercise (> 8 hours of continuous exercise per week); weighed over 400 pounds; or used antibiotics or probiotics in the past 3 months.

All procedures complied with institutional guidelines and were approved by the Institutional Review Board at UCLA's Office of Protection for Research Subjects. All participants provided written informed consent.

Study design

In this cross-sectional study, all participants underwent multimodal MRI brain imaging, provided a stool sample within 2-3 days prior to scans, and answered questionnaires including detailed diet information during the week before the MRI scan (consistent with published studies[90–95]). This study was a secondary data analysis on existing data and was pooled from two studies: (IRB#s 16-000281, 16-000187).

Questionnaires

Questionnaire data included the following: *Resilience* was measured using the Connor-Davidson Resilience Scale (CD-RISC), which is a self-reported scale that consists of 25 items, evaluated on a five-point Likert scale ranging from 0-4; not true at all (0), rarely true (1), sometimes true (2), often true (3), and true nearly all the time (4) resulting in a number between 0-100 with higher scores indicating higher resilience. The resilience total score is comprised of 5 factors: 1) personal competence, high standards, and tenacity; 2) trust in one's instincts, tolerance of negative affect, and strengthening effects of stress; 3) positive acceptance of change and secure relationships; 4) control; 5) spiritual influences[4]. The mean resilience score of the general US population is 80.7. However, given our study's participants having a median body mass index (BMI) of 28.06, we based the threshold for high and low resilience using the mean score (83.1) of a study involving mostly overweight patients (normally distributed data with Cronbach's alpha of 0.92)[96]. In this study, a CD-RISC score ≥ 83.1 was labeled as "High" resilience (N = 50) and < 83.1 was "Low" Resilience.

Other measures included BMI, socioeconomic status (SES), Early Trauma Inventory (ETI)[97], Adverse Childhood Experiences (ACE) questionnaire[98], Hospital Anxiety and Depression Scale (HADS)[60], Coping Strategies Questionnaire (CSQ)[99], Perceived Stress Scale (PSS)[100], State-Trait Anxiety Inventory (STAI)[61], Positive and Negative Affect Schedule (PANAS)[101], 12-item Short Form (SF12) Survey[102], International Physical Activity Questionnaires (IPAQ)[103,104], Behavioral Inhibition System, Behavioral Approach System (BISBAS)[105], Everyday Discrimination Score (EDS)[106,107], Brief COPE (BCope)[108], Patient Health Questionnaire (PHQ)[109], Multiple Ability Self-Report Questionnaire (MASQ)[62], Mindful Attention Awareness Scale (MAAS)[110], Five Facet Mindfulness (FFM)[59], Patient-Reported Outcomes Measurement Information System Sleep Scale (PROMIS_Sleep9)[111], Visceral Sensitivity Index (VSI)[112,113], Pain Vigilance and Awareness Questionnaire (PVAQ)[114], Pain Catastrophizing Scale (PCS)[115,116], Normal Personality Assessment (NEO)[117,118], International Personality Pool (IPIP)[58], Diet Questionnaire (used in our previous studies)[93].

Gut Microbiome

The methods used for sample collection, processing and analysis are described in detail in published papers[119,120].

Collection and storage

Participants were given “at-home kits” with specified instructions for when to collect and how to store their stool sample. Stool was collected 2-3 days before the MRI scan. 2-3 consecutive diet diaries were collected from the time of enrollment to the time of the MRI scan and stool collection (1-2 weekdays and 1 weekend). Participants were asked to collect the stool before the first meal of the day and immediately freeze the fresh stool after collection. If participants were on antidiarrheal or laxatives, they were asked to refrain from use for 2-3 days before the sample collection. Any deviations from the stool sample collection were documented to account for in the analysis. Fecal samples were stored at −80°C, then ground to coarse powder by mortar and pestle under liquid nitrogen and aliquoted for nucleic acid extraction and metabolomic profiling.

Fecal microbial profiling

DNA extraction with bead beating was performed using the QIAGEN Powersoil DNA Isolation Kit (MO BIO Laboratories, Carlsbad, CA), following the manufacturer’s protocol. The V4 hypervariable region of the 16S rRNA gene was then amplified using 515F and 806R primers to generate a sequencing library according to a published protocol[121]. The PCR products were purified with a commercial kit. The library underwent 2x250 sequencing on an Illumina HiSeq 2500 to a mean depth of 250,000 merged sequences per sample. The DADA2 pipeline was used for quality filtering, merging paired-end reads, removing chimera, and assigning taxonomy to each amplicon sequence variant (ASV) using the SILVA 138 reference database[122–125].

Alpha and Beta Diversity.—Bacterial counts were derived using the DADA2 package v1. 29.0[122] and analyzed using R statistical software. To preserve statistical power, only bacterial genera that were present in at least 10% of the samples were included in analyses resulting in the exclusion of 146 genera and inclusion of 125 genera for analyses. Microbial alpha diversity was assessed on datasets rarefied to 10000 using the Shannon index to assess richness and evenness. Permutational analysis of variance analyses (PERMANOVA) of Bray-Curtis dissimilarities was used to quantify variation in genus between groups. Specifically, beta diversity was calculated using the adonis2 function in Vegan package 2.6-4 to determine Bray-Curtis distance matrices and conduct PERMANOVA significance testing for compositional data with 999 permutations.

Fecal metabolomics processing

Aliquots of fecal samples were shipped to and processed by Metabolon, Inc and run as a single batch through their global HD4 Metabolomics platform[126], which involves running methanol-extracted samples through ultrahigh performance liquid chromatography-tandem mass spectroscopy under four separate chromatography and electrospray ionization conditions, separating the compounds by their chemical properties. The amount of missing data was low (<3%). However, missing values in the raw data were median imputed using median values, and ineffective peaks were dropped through interquartile range denoising, and an internal standardization normalization method was employed. The metabolites data block was compiled from the metabolite profiling results, and a 3-dimensional matrix with

metabolite numbers, sample names, and normalized peak intensities processed with the MetaboAnlyst web software 3.0 (http://www.metaboanalyst.ca).

Fecal Transcriptomics Processing

Fecal samples were submitted to Viome Life Sciences, Inc., where RNA extraction, metatranscriptomics sequencing and annotation were conducted. A detailed description of these procedures is provided in previously published work[127]. In sum, RNA extraction by beading was performed, DNA degraded by DNase, and 16S/23S ribosomal RNA depleted by subtractive hybridization. Sequencing libraries were prepared from the resulting RNA and underwent 150x2 paired-end sequencing on Illumina NovaSeq. Taxonomy was assigned by aligning sequencing reads to a precomputed database of unique k-mers; 898 taxa were identified, including bacteria, fungi, viruses, and bacteriophages. Functional annotation was performed by aligning sequencing reads to the integrated gene catalog from the MetaHIT consortium then mapping these genes to the KEGG database; 5,896 distinct transcripts annotated as KOs were identified[128].

Multimodal neuroimaging

Magnetic resonance imaging acquisition.—Each subject underwent imaging in a 3.0T Prisma MRI Scanner with a 20-channel head coil (Siemens Healthcare, Erlangen, Germany) for a high resolution T1 structural scan, a resting state functional scan, and a diffusion weighted scan. Participants were asked to fast for an average of 6 hours prior to scanning. The acquisition parameters are as follows: T1 weighted MP-RAGE scans acquired to assess brain structure (TR: 2300ms, TE: 2.98ms, TI: 900ms, flip angle: 9°, field of view: 240 x 256 mm, acquisition matrix: 240 x 256, slice thickness: 1 mm, voxel resolution: 1 x 1 x 1 mm). A 10-minute resting-state fMRI scan was acquired to assess resting-state functional connectivity (TR: 2000ms, TE: 28ms, flip angle: 77°, acquisition matrix: 64 x 64, slice thickness: 4 mm, voxel resolution: 3.44 x 3.44 x 4 mm, 300 volumes). A diffusion weighted image was acquired to assess white matter anatomical connectivity (64 noncollinear directions, b = 1000 s/mm2, 9 b = 0 s/mm2 images, TR: 9500ms, TE: 88ms, field of view: 2304 x 2304, acquisition matrix: 128 x 128, slice thickness: 2mm, spacing between slices: 2mm).

MRI preprocessing. —Scans from each neuroimaging modality was considered as separate datasets and processed separately with the appropriate respective modality specific pipelines. Structural scans were processed and passed quality control using Statistical Parametric Mapping 12.[129] Processing included motion correction, skull stripping, segmentation into gray matter, white matter, and cerebral spinal fluid (CSF), and normalization onto a NMI153 T1 template.

Structural image processing.—Cortical reconstruction and volumetric segmentation was done using the FreeSurfer6 analysis suite[130]. All participants' T1 structural data was first parcellated using the Destrieux cortical atlas[131] and the Harvard-Oxford subcortical atlas and the Harvard Ascending Arousal Network (AAN)[132]. FreeSurfer was used to compute values of cortical thickness, surface area, mean curvature and volume for cortical

ROIs and volume for subcortical ROIs. Multimodal scans were processed similar to previously published studies[95,133–135].

Functional image processing.—Functional scans were preprocessed using the volume-based rs-FC analysis pipeline in the functional connectivity toolbox (CONN)[136]. All scans underwent realignment and unwarping, slice-timing correction, and outlier identification (advanced retrospective technique-based identification of outlier scans, ART) for scrubbing. Functional and structural data (T1 scans) were normalized and segmented into grey matter, white matter and CSF tissue[137]. Denoising was done using ordinary least squares regression of potential confounding effects and temporal band-pass filtering. The default anatomical component-based noise correction procedure (aCompCor) includes noise components from white matter[138], estimated subject-motion parameters[139], outlier scans or scrubbing based on frame-wise displacement[140], and effect of rest repressing potential ramping effects (at the start of the session)[141]. The influence of physiological, head-motion and other noise sources were minimized using a 0.008 Hz to 0.09 Hz after regression temporal band-pass filter[142]. Fisher transformed correlations (Z) were computed between the functional time series of all the FreeSurfer parcellated regions to derive a 165x165 matrix for each participant. A single vector representing the correlation strength between each ROI pair was concatenated from the bottom half of the undirected matrix for each subject.

Diffusion image processing.—Diffusion-weighted images, corrected for eddy current-induced distortions and movement with FSL's *eddy_correct* tool[143], along with the associated b-vectors and v-values were converted into Camino data formats with Camino's *fsl2scheme* and *image2voxel*[144]. Weighted linear least squares regression was used to fit a diffusion tensor on the voxel order data in Camino (*wdtfit*)[144]. Deterministic and probabilistic tensor-based approaches have shown to have similar performance[145]. The track command in Camino Euler algorithm performed whole-brain deterministic tractography with a step size of 0.5 and curve threshold of 76. Connectivity matrices were constructed using the *conmat* command in Camino and produced a 165x165 matrix that represents the number of streamlines connecting each ROI-to-ROI pair. Every subject's matrix went through within-subject normalization by taking a sum of all counts between each ROI, then dividing each pair's count by that total. The bottom half of the undirected matrix was then concatenated into one vector for each subject representing every ROI pair.

Data Integration Analysis for Biomarker discover using Latent cOmponents (DIABLO)

Approach Overview.—Integrating multiple omics approaches is essential for a thorough understanding of stress resilience and its associated phenotypes. Studying multimodal brain imaging, microbiome, transcriptome, metabolome, and clinical/behavioral variables in isolation cannot provide a comprehensive biological insight. DIABLO[146] facilitates employing integrative multi-omics analysis, examining the interplay between various datasets to unravel the intricacies of stress-resilient phenotypes.

We used DIABLO to accomplish our Integrative Multi-omics Analyses goal to elucidate the interactions among central (brain), peripheral (microbiome, metabolome), and clinical/behavioral markers linked to resilience phenotypes. This advanced multi-block integration

strategy simultaneously models outcomes based on multiple data matrices, identifies key predictive variables, and unveils relationships between different dataset types. DIABLO calculates linear combinations (multi-omic signatures) maximally correlated with a specified outcome while performing variable selection, controlling for relevant covariates (e.g., gender, age, BMI), and correcting for multiple comparisons. The result is a yield of a minimal subset of variables associated with resilience outcomes. Additionally, we identify a limited number of multi-omics signatures distinguishing high resilience from low resilience in both training and test sets.

DIABLO Analysis.—DIABLO[146] with a supervised learning framework was conducted to determine a sparse subset of correlated phenotypic and behavioral features from the 6 high-dimensional input data blocks (Q) that predict resilience group given the 83.1 score threshold[96]. Data was split into a 70% training (N = 81) and 30% testing set (N = 35). Training data is used to calculate the design matrix and train the model. DIABLO extends sparse generalized canonical correlation analysis, a generalization of partial least squares (PLS)[146,147], to a supervised machine learning framework with scarcity constraints for variable selection. Pairwise sparse PLS (sPLS) models were run (e.g. clinical versus resting-state functional MRI; metabolome versus diffusion MRI) prior to the DIABLO analysis to gauge the overall correlation structure between the dataset types and guide the data integration in DIABLO[146]. A weighted Q x Q design matrix, a DIABLO input that informs the integration process, was calculated taking the correlation of the first principal component of individual sPLS models between pairwise data blocks. The data-driven design matrix contains values from 0 to 1 and represents *if and by how much* each data block Q should be correlated to one another. The final model consists of a limited number of features across datatypes that show high correlation with one another, which gives insight to both which 'omic types' are relevant to the discriminatory process and how different 'omic types,' or datasets interact with one another.

Data Preparation.—Following the independent processing of the six data blocks (clinical, microbiome, metabolite, morphological MRI, rs-FC MRI, DTI MRI), involved the examination of each block to eliminate variables not suitable for analysis. Due to the nature of the data integration algorithm, variables exhibiting near zero variance (NZV) were detected and excluded from further consideration. Regarding the clinical dataset, categorical variables of interest were replaced with dummy variables before identifying and 16 variables with NZV were eliminated. For the fecal metabolome dataset, 38 NZV variables were dropped before performing median normalization. All clinical and metabolome variables with 50% or more NA's were removed.

Neuroimaging data preparation for DIABLO.—Measures of brain morphometry, resting state functional connectivity and anatomical connectivity were derived for each individual and pairwise ROI similar to our previous published studies[131,148–151]. Data from the three neuroimaging modalities was considered as separate datasets and went through their own specific preprocessing methods. To construct the structural MRI dataset, the observations that used the ascending arousal network (AAN) and Destrieux Harvard-Oxford atlas parcellations were merged and measures of surface area and volume were residualized

by the estimated total intracranial volume (eTIV) to control for effects driven by brain size[152–154]. The NZV features in the resting-state functional MRI and diffusion MRI dataset, which can consist of many variables with zeros (i.e., regions that do not share anatomic connections), were dropped. Data blocks for all three neuroimaging datasets were resilience group median imputed.

The final clinical dataset had 99 features, metabolome dataset had 714 features, transcriptome dataset had 1,424 features, structural MRI dataset had 626 features, resting-state functional MRI dataset had 15,753 features, and diffusion MRI dataset had 3,408 features. All six datasets were then scaled and centered separately by calculating mean and standard deviation of each vector, then "scaling" each element by subtracting the mean and dividing by the standard deviation within the DIABLO function call. These datasets were used in subsequent analyses.

Variable selection.—An initial DIABLO model with 10 components and all features from each dataset was fit on the training subset and the global performance was assessed with 5-fold cross validation to identify the number of components that produces the lowest Balanced Error Rate (BER) with mahalanobis distance. One component produced the lowest BER. Mahalanobis distance was set as the distance metric parameter as it is robust at handling imbalanced groups[155]. Manual tuning was then performed to determine the optimal number of variables for each data block for the selected number of components to obtain the lowest BER on the unseen test subset. The testing set's performance was used to determine the final model. DIABLO outputs a set of components (i.e., latent variables), a set of loading vectors (i.e., coefficients assigned to each variable) and a subset of selected variables in each dataset associated with each component. The outputs are obtained by maximizing the covariance between a linear combination of X variables and Y labels and the magnitude of the loading vectors represents the importance of that variable in the model with higher values suggesting greater importance[146,147]. Loading plots show the importance of each variable within each component. Connectograms represent the correlation between variables from each datatype selected by the final DIABLO model. Performance metrics, including a confusion matrix, BER, and area under the receiver operating characteristic curve (AUC) curve were calculated to determine how well the model performed for each data block and overall. AUC is a value ranging from 0 to 1 that summarizes the overall diagnostic accuracy of a model. 1 represents a perfectly accurate classification model, 0.5 represents a poor model with no discriminatory ability, and values between 0.7 and 0.8 are considered acceptable[156].

Spearman Correlations.—Spearman correlations were conducted to calculate associations between the five factors that compose the total resilience score and DIABLO selected variables.

Supplementary Material

Refer to Web version on PubMed Central for supplementary material.

Acknowledgements:

This research was supported by grants from the National Institutes of Health including R01 MD015904 (AG), K23 DK106528 (AG), R03 DK121025 (AG), ULTR001881/DK041301 (UCLA CURE/CTSI Pilot and Feasibility Study (AG); and pilot funds provided for brain scanning by the Ahmanson-Lovelace Brain Mapping Center. These funders played no role in study design, or the collection, analysis, and interpretation of the data. We acknowledge the analytical and data curation efforts provided by the Neuroimaging Core, the Integrative Biostatistics and Bioinformatics Core, and the Database and Clinical Core of the Goodman-Luskin Microbiome Center at UCLA.

Data Availability:

Deidentified individual participant data (brain) can be shared upon request and will be made available through the Center's pain repository portal (https://www.painrepository.org/). To access the data, participants will fill out a user agreement, upon which access to the data will be made available through a secure password protected portal. The raw microbiome sequences can be accessed NIH NCBI BioProject (BioProject ID: PRJNA946906).

References

1. American Institute of Stress. (2013).
2. Vella S-LC & Pai NB A Theoretical Review of Psychological Resilience: Defining Resilience and Resilience Research over the Decades. Archives of Medicine and Health Sciences 7 (2019).
3. Hill Y, Den Hartigh RJR, Meijer RR, De Jonge P & Van Yperen NW The temporal process of resilience. Sport, Exercise, and Performance Psychology 7, 363–370, doi:10.1037/spy0000143 (2018).
4. Connor KM & Davidson JR Development of a new resilience scale: the Connor-Davidson Resilience Scale (CD-RISC). Depress Anxiety 18, 76–82, doi:10.1002/da.10113 (2003). [PubMed: 12964174]
5. Ahmed Z & Julius SH Academic performance, resilience, depression, anxiety and stress among women college students. Indian Journal of Positive Psychology 6, 367–370 (2015).
6. Poudel-Tandukar K. et al. Resilience and anxiety or depression among resettled Bhutanese adults in the United States. Int J Soc Psychiatry 65, 496–506, doi:10.1177/0020764019862312 (2019). [PubMed: 31288604]
7. Harker R, Pidgeon AM, Klaassen F & King S Exploring resilience and mindfulness as preventative factors for psychological distress burnout and secondary traumatic stress among human service professionals. Work 54, 631–637, doi:10.3233/WOR-162311 (2016). [PubMed: 27286075]
8. Eisen SV et al. Postdeployment resilience as a predictor of mental health in operation enduring freedom/operation iraqi freedom returnees. Am J Prev Med 47, 754–761, doi:10.1016/j.amepre.2014.07.049 (2014). [PubMed: 25455117]
9. Uliaszek AA et al. The role of neuroticism and extraversion in the stress-anxiety and stress-depression relationships. Anxiety Stress Coping 23, 363–381, doi:10.1080/10615800903377264 (2010). [PubMed: 19890753]
10. Polizzi CP & Lynn SJ Regulating Emotionality to Manage Adversity: A Systematic Review of the Relation Between Emotion Regulation and Psychological Resilience. Cognitive Ther Res 45, 577–597, doi:10.1007/s10608-020-10186-1 (2021).
11. Allott KA et al. The impact of neuropsychological functioning and coping style on perceived stress in individuals with first-episode psychosis and healthy controls. Psychiatry Res 226, 128–135, doi:10.1016/j.psychres.2014.12.032 (2015). [PubMed: 25618467]
12. Sippel LM, Pietrzak RH, Charney DS, Mayes LC & Southwick SM How does social support enhance resilience in the trauma-exposed individual? Ecology and Society 20, art10, doi:10.5751/es-07832-200410 (2015).
13. Carney RM et al. Change in heart rate and heart rate variability during treatment for depression in patients with coronary heart disease. Psychosom Med 62, 639–647, doi:10.1097/00006842-200009000-00007 (2000). [PubMed: 11020093]

14. Sydnor VJ et al. Neurodevelopment of the association cortices: Patterns, mechanisms, and implications for psychopathology. Neuron 109, 2820–2846, doi:10.1016/j.neuron.2021.06.016 (2021). [PubMed: 34270921]
15. Turnbaugh PJ et al. The human microbiome project. Nature 449, 804–810, doi:10.1038/nature06244 (2007). [PubMed: 17943116]
16. Jiang H. et al. Altered fecal microbiota composition in patients with major depressive disorder. Brain Behav Immun 48, 186–194, doi:10.1016/j.bbi.2015.03.016 (2015). [PubMed: 25882912]
17. Jiang HY et al. Altered gut microbiota profile in patients with generalized anxiety disorder. J Psychiatr Res 104, 130–136, doi:10.1016/j.jpsychires.2018.07.007 (2018). [PubMed: 30029052]
18. He Y. et al. Gut microbiome and magnetic resonance spectroscopy study of subjects at ultra-high risk for psychosis may support the membrane hypothesis. Eur Psychiatry 53, 37–45, doi:10.1016/j.eurpsy.2018.05.011 (2018). [PubMed: 29870894]
19. Butler MI et al. The gut microbiome in social anxiety disorder: evidence of altered composition and function. Transl Psychiatry 13, 95, doi:10.1038/s41398-023-02325-5 (2023). [PubMed: 36941248]
20. Evans SJ et al. The gut microbiome composition associates with bipolar disorder and illness severity. J Psychiatr Res 87, 23–29, doi:10.1016/j.jpsychires.2016.12.007 (2017). [PubMed: 27988330]
21. Kang DW et al. Reduced incidence of Prevotella and other fermenters in intestinal microflora of autistic children. PLoS One 8, e68322, doi:10.1371/journal.pone.0068322 (2013). [PubMed: 23844187]
22. Foster JA & McVey Neufeld KA Gut-brain axis: how the microbiome influences anxiety and depression. Trends Neurosci 36, 305–312, doi:10.1016/j.tins.2013.01.005 (2013). [PubMed: 23384445]
23. Mayer EA The neurobiology of stress and gastrointestinal disease. Gut 47, 861–869, doi:10.1136/gut.47.6.861 (2000). [PubMed: 11076888]
24. Bear T. et al. The Microbiome-Gut-Brain Axis and Resilience to Developing Anxiety or Depression under Stress. Microorganisms 9, 723, doi:10.3390/microorganisms9040723 (2021). [PubMed: 33807290]
25. Cryan JF & Dinan TG Mind-altering microorganisms: the impact of the gut microbiota on brain and behaviour. Nat Rev Neurosci 13, 701–712, doi:10.1038/nrn3346 (2012). [PubMed: 22968153]
26. Parashar A & Udayabanu M Gut microbiota regulates key modulators of social behavior. Eur Neuropsychopharmacol 26, 78–91, doi:10.1016/j.euroneuro.2015.11.002 (2016). [PubMed: 26613639]
27. Yang C. et al. Bifidobacterium in the gut microbiota confer resilience to chronic social defeat stress in mice. Scientific reports 7, 45942, doi:10.1038/srep45942 (2017). [PubMed: 28368029]
28. Li LF et al. Increased Lactobacillus Abundance Contributes to Stress Resilience in Mice Exposed to Chronic Social Defeat Stress. Neuroendocrinology 113, 563–576, doi:10.1159/000528876 (2023). [PubMed: 36587608]
29. Wang X et al. Abnormal compositions of gut microbiota and metabolites are associated with susceptibility versus resilience in rats to inescapable electric stress. Journal of affective disorders 331, 369–379, doi:10.1016/j.jad.2023.03.073 (2023). [PubMed: 36972851]
30. Zhang K et al. Abnormal composition of gut microbiota is associated with resilience versus susceptibility to inescapable electric stress. Transl Psychiatry 9, 231, doi:10.1038/s41398-019-0571-x (2019). [PubMed: 31530799]
31. Kanehisa M, Furumichi M, Tanabe M, Sato Y & Morishima K KEGG: new perspectives on genomes, pathways, diseases and drugs. Nucleic Acids Res 45, D353–D361, doi:10.1093/nar/gkw1092 (2017). [PubMed: 27899662]
32. Barrett E, Ross RP, O'Toole PW, Fitzgerald GF & Stanton C gamma-Aminobutyric acid production by culturable bacteria from the human intestine. J Appl Microbiol 113, 411–417, doi:10.1111/j.1365-2672.2012.05344.x (2012). [PubMed: 22612585]
33. Baj A et al. Glutamatergic Signaling Along The Microbiota-Gut-Brain Axis. Int J Mol Sci 20, doi:10.3390/ijms20061482 (2019).

34. O'Mahony SM, Clarke G, Borre YE, Dinan TG & Cryan JF Serotonin, tryptophan metabolism and the brain-gut-microbiome axis. Behav Brain Res 277, 32–48, doi:10.1016/j.bbr.2014.07.027 (2015). [PubMed: 25078296]
35. Cryan JF et al. The Microbiota-Gut-Brain Axis. Physiol Rev 99, 1877–2013, doi:10.1152/physrev.00018.2018 (2019). [PubMed: 31460832]
36. Rosso IM et al. Insula and anterior cingulate GABA levels in posttraumatic stress disorder: preliminary findings using magnetic resonance spectroscopy. Depress Anxiety 31, 115–123, doi:10.1002/da.22155 (2014). [PubMed: 23861191]
37. Murrough JW et al. Reduced amygdala serotonin transporter binding in posttraumatic stress disorder. Biol Psychiatry 70, 1033–1038, doi:10.1016/j.biopsych.2011.07.003 (2011). [PubMed: 21855859]
38. Bonaz B, Bazin T & Pellissier S The Vagus Nerve at the Interface of the Microbiota-Gut-Brain Axis. Front Neurosci 12, 49, doi:10.3389/fnins.2018.00049 (2018). [PubMed: 29467611]
39. Miller TL & Wolin MJ Pathways of acetate, propionate, and butyrate formation by the human fecal microbial flora. Appl Environ Microbiol 62, 1589–1592, doi:10.1128/aem.62.5.1589-1592.1996 (1996). [PubMed: 8633856]
40. Stilling RM et al. The neuropharmacology of butyrate: The bread and butter of the microbiota-gut-brain axis? Neurochem Int 99, 110–132, doi:10.1016/j.neuint.2016.06.011 (2016). [PubMed: 27346602]
41. Bharwani A et al. Structural & functional consequences of chronic psychosocial stress on the microbiome & host. Psychoneuroendocrinology 63, 217–227, doi:10.1016/j.psyneuen.2015.10.001 (2016). [PubMed: 26479188]
42. Tanelian A, Nankova B, Miari M, Nahvi RJ & Sabban EL Resilience or susceptibility to traumatic stress: Potential influence of the microbiome. Neurobiol Stress 19, 100461, doi:10.1016/j.ynstr.2022.100461 (2022). [PubMed: 35789769]
43. Sampson TR & Mazmanian SK Control of brain development, function, and behavior by the microbiome. Cell Host Microbe 17, 565–576, doi:10.1016/j.chom.2015.04.011 (2015). [PubMed: 25974299]
44. Tillisch K et al. Brain Structure and Response to Emotional Stimuli as Related to Gut Microbial Profiles in Healthy Women. Psychosom Med 79, 905–913, doi:10.1097/PSY.0000000000000493 (2017). [PubMed: 28661940]
45. Kohn N et al. Multivariate associative patterns between the gut microbiota and large-scale brain network connectivity. Gut Microbes 13, 2006586, doi:10.1080/19490976.2021.2006586 (2021). [PubMed: 34856861]
46. Tillisch K et al. Consumption of fermented milk product with probiotic modulates brain activity. Gastroenterology 144, 1394–1401, 1401 e1391-1394, doi:10.1053/j.gastro.2013.02.043 (2013). [PubMed: 23474283]
47. Tabibnia G An affective neuroscience model of boosting resilience in adults. Neurosci Biobehav Rev 115, 321–350, doi:10.1016/j.neubiorev.2020.05.005 (2020). [PubMed: 32522489]
48. Christoff K, Irving ZC, Fox KC, Spreng RN & Andrews-Hanna JR Mind-wandering as spontaneous thought: a dynamic framework. Nat Rev Neurosci 17, 718–731, doi:10.1038/nrn.2016.113 (2016). [PubMed: 27654862]
49. Hamilton JP et al. Default-mode and task-positive network activity in major depressive disorder: implications for adaptive and maladaptive rumination. Biol Psychiatry 70, 327–333, doi:10.1016/j.biopsych.2011.02.003 (2011). [PubMed: 21459364]
50. Shaurya Prakash R, De Leon AA, Klatt M, Malarkey W & Patterson B Mindfulness disposition and default-mode network connectivity in older adults. Soc Cogn Affect Neurosci 8, 112–117, doi:10.1093/scan/nss115 (2013). [PubMed: 23051900]
51. Gupta A et al. Morphological brain measures of cortico-limbic inhibition related to resilience. J Neurosci Res 95, 1760–1775, doi:10.1002/jnr.24007 (2017). [PubMed: 28029706]
52. Helpman L et al. Ptsd Remission after Prolonged Exposure Treatment Is Associated with Anterior Cingulate Cortex Thinning and Volume Reduction. Depress Anxiety 33, 384–391, doi:10.1002/da.22471 (2016). [PubMed: 26864570]

53. Kong F, Wang X, Hu S & Liu J Neural correlates of psychological resilience and their relation to life satisfaction in a sample of healthy young adults. Neuroimage 123, 165–172, doi:10.1016/j.neuroimage.2015.08.020 (2015). [PubMed: 26279212]
54. Doucet GE, Bassett DS, Yao N, Glahn DC & Frangou S The Role of Intrinsic Brain Functional Connectivity in Vulnerability and Resilience to Bipolar Disorder. Am J Psychiatry 174, 1214–1222, doi:10.1176/appi.ajp.2017.17010095 (2017). [PubMed: 28817956]
55. Ke J et al. A longitudinal fMRI investigation in acute post-traumatic stress disorder (PTSD). Acta Radiol 57, 1387–1395, doi:10.1177/0284185115585848 (2016). [PubMed: 25995310]
56. Admon R et al. Imbalanced neural responsivity to risk and reward indicates stress vulnerability in humans. Cereb Cortex 23, 28–35, doi:10.1093/cercor/bhr369 (2013). [PubMed: 22291028]
57. Schmidt AT et al. Diffusion Tensor Imaging Correlates of Resilience Following Adolescent Traumatic Brain Injury. Cogn Behav Neurol 34, 259–274, doi:10.1097/WNN.0000000000000283 (2021). [PubMed: 34851864]
58. Goldberg LR et al. The international personality item pool and the future of public-domain personality measures. Journal of Research in Personality 40, 84–96, doi:10.1016/j.jrp.2005.08.007 (2006).
59. Baer RA, Smith GT, Hopkins J, Krietemeyer J & Toney L Using self-report assessment methods to explore facets of mindfulness. Assessment 13, 27–45, doi:10.1177/1073191105283504 (2006). [PubMed: 16443717]
60. Zigmond AS & Snaith RP The hospital anxiety and depression scale. Acta Psychiatr Scand 67, 361–370, doi:10.1111/j.1600-0447.1983.tb09716.x (1983). [PubMed: 6880820]
61. Julian LJ Measures of anxiety: State-Trait Anxiety Inventory (STAI), Beck Anxiety Inventory (BAI), and Hospital Anxiety and Depression Scale-Anxiety (HADS-A). Arthritis Care Res (Hoboken) 63 Suppl 11, S467–472, doi:10.1002/acr.20561 (2011). [PubMed: 22588767]
62. Seidenberg M, Haltiner A, Taylor MA, Hermann BB & Wyler A Development and validation of a Multiple Ability Self-Report Questionnaire. J Clin Exp Neuropsychol 16, 93–104, doi:10.1080/01688639408402620 (1994). [PubMed: 8150893]
63. Gonzalez I, Cao KA, Davis MJ & Dejean S Visualising associations between paired ‘omics’ data sets. Biodata Min 5, 19, doi:10.1186/1756-0381-5-19 (2012). [PubMed: 23148523]
64. Garcia-Martinez P et al. Perceived Stress in Relation to Quality of Life and Resilience in Patients with Advanced Chronic Kidney Disease Undergoing Hemodialysis. Int J Environ Res Public Health 18, doi:10.3390/ijerph18020536 (2021).
65. Creswell JD Mindfulness Interventions. Annu Rev Psychol 68, 491–516, doi:10.1146/annurev-psych-042716-051139 (2017). [PubMed: 27687118]
66. Hildebrandt LK, McCall C, Engen HG & Singer T Cognitive flexibility, heart rate variability, and resilience predict fine-grained regulation of arousal during prolonged threat. Psychophysiology 53, 880–890, doi:10.1111/psyp.12632 (2016). [PubMed: 26899260]
67. Martindale SL et al. Neuropsychological functioning, coping, and quality of life among returning war veterans. Rehabil Psychol 61, 231–239, doi:10.1037/rep0000076 (2016). [PubMed: 26891248]
68. Rutherford ST & Bassler BL Bacterial quorum sensing: its role in virulence and possibilities for its control. Cold Spring Harb Perspect Med 2, a012427, doi:10.1101/cshperspect.a012427 (2012). [PubMed: 23125205]
69. Caldovic L & Tuchman M N-acetylglutamate and its changing role through evolution. Biochem J 372, 279–290, doi:10.1042/BJ20030002 (2003). [PubMed: 12633501]
70. Bowerman KL et al. Disease-associated gut microbiome and metabolome changes in patients with chronic obstructive pulmonary disease. Nat Commun 11, 5886, doi:10.1038/s41467-020-19701-0 (2020). [PubMed: 33208745]
71. Li JY et al. Arginine metabolism regulates the pathogenesis of inflammatory bowel disease. Nutr Rev 81, 578–586, doi:10.1093/nutrit/nuac070 (2023). [PubMed: 36040377]
72. Graber CD, Goust JM, Glassman AD, Kendall R & Loadholt CB Immunomodulating properties of dimethylglycine in humans. J Infect Dis 143, 101–105, doi:10.1093/infdis/143.1.101 (1981). [PubMed: 6163829]

73. Wang Z, Shao D, Wu S, Song Z & Shi S Heat stress-induced intestinal barrier damage and dimethylglycine alleviates via improving the metabolism function of microbiota gut brain axis. Ecotoxicol Environ Saf 244, 114053, doi:10.1016/j.ecoenv.2022.114053 (2022). [PubMed: 36084503]
74. Hamani C et al. The subcallosal cingulate gyrus in the context of major depression. Biol Psychiatry 69, 301–308, doi:10.1016/j.biopsych.2010.09.034 (2011). [PubMed: 21145043]
75. Etkin A, Egner T & Kalisch R Emotional processing in anterior cingulate and medial prefrontal cortex. Trends in cognitive sciences 15, 85–93, doi:10.1016/j.tics.2010.11.004 (2011). [PubMed: 21167765]
76. Rode J et al. Probiotic Mixture Containing Lactobacillus helveticus, Bifidobacterium longum and Lactiplantibacillus plantarum Affects Brain Responses Toward an Emotional Task in Healthy Subjects: A Randomized Clinical Trial. Front Nutr 9, 827182, doi:10.3389/fnut.2022.827182 (2022). [PubMed: 35571902]
77. Rode J et al. Multi-Strain Probiotic Mixture Affects Brain Morphology and Resting State Brain Function in Healthy Subjects: An RCT. Cells 11, doi:10.3390/cells11182922 (2022).
78. Uhr L, Tsolaki E & Pouratian N Diffusion tensor imaging correlates of depressive symptoms in Parkinson disease. J Comp Neurol 530, 1729–1738, doi:10.1002/cne.25310 (2022). [PubMed: 35152429]
79. Montag C, Reuter M, Weber B, Markett S & Schoene-Bake JC Individual differences in trait anxiety are associated with white matter tract integrity in the left temporal lobe in healthy males but not females. Neuroscience 217, 77–83, doi:10.1016/j.neuroscience.2012.05.017 (2012). [PubMed: 22609931]
80. Amico F et al. Structural MRI correlates for vulnerability and resilience to major depressive disorder. J Psychiatry Neurosci 36, 15–22, doi:10.1503/jpn.090186 (2011). [PubMed: 20964952]
81. Williams LM et al. Arousal dissociates amygdala and hippocampal fear responses: evidence from simultaneous fMRI and skin conductance recording. Neuroimage 14, 1070–1079, doi:10.1006/nimg.2001.0904 (2001). [PubMed: 11697938]
82. Butler T et al. Human fear-related motor neurocircuitry. Neuroscience 150, 1–7, doi:10.1016/j.neuroscience.2007.09.048 (2007). [PubMed: 17980493]
83. Feeny NC, Zoellner LA, Fitzgibbons LA & Foa EB Exploring the roles of emotional numbing, depression, and dissociation in PTSD. J Trauma Stress 13, 489–498, doi:10.1023/a:1007789409330 (2000). [PubMed: 10948488]
84. Roeckner AR, Oliver KI, Lebois LAM, van Rooij SJH & Stevens JS Neural contributors to trauma resilience: a review of longitudinal neuroimaging studies. Transl Psychiatry 11, 508, doi:10.1038/s41398-021-01633-y (2021). [PubMed: 34611129]
85. Patel R, Spreng RN, Shin LM & Girard TA Neurocircuitry models of posttraumatic stress disorder and beyond: a meta-analysis of functional neuroimaging studies. Neurosci Biobehav Rev 36, 2130–2142, doi:10.1016/j.neubiorev.2012.06.003 (2012). [PubMed: 22766141]
86. Peng L, Li ZR, Green RS, Holzman IR & Lin J Butyrate enhances the intestinal barrier by facilitating tight junction assembly via activation of AMP-activated protein kinase in Caco-2 cell monolayers. J Nutr 139, 1619–1625, doi:10.3945/jn.109.104638 (2009). [PubMed: 19625695]
87. Lewis K et al. Enhanced translocation of bacteria across metabolically stressed epithelia is reduced by butyrate. Inflamm Bowel Dis 16, 1138–1148, doi:10.1002/ibd.21177 (2010). [PubMed: 20024905]
88. Maes M, Kubera M & Leunis JC The gut-brain barrier in major depression: intestinal mucosal dysfunction with an increased translocation of LPS from gram negative enterobacteria (leaky gut) plays a role in the inflammatory pathophysiology of depression. Neuro Endocrinol Lett 29, 117–124 (2008). [PubMed: 18283240]
89. Forsythe P, Bienenstock J & Kunze WA Vagal pathways for microbiome-brain-gut axis communication. Adv Exp Med Biol 817, 115–133, doi:10.1007/978-1-4939-0897-4_5 (2014). [PubMed: 24997031]
90. Jacobs JP et al. Cognitive behavioral therapy for irritable bowel syndrome induces bidirectional alterations in the brain-gut-microbiome axis associated with gastrointestinal symptom improvement. Microbiome 9, 236, doi:10.1186/s40168-021-01188-6 (2021). [PubMed: 34847963]

91. Jacobs JP et al. Multi-omics profiles of the intestinal microbiome in irritable bowel syndrome and its bowel habit subtypes. Microbiome 11, 5, doi:10.1186/s40168-022-01450-5 (2023). [PubMed: 36624530]
92. Dong TS et al. A Distinct Brain-Gut-Microbiome Profile Exists for Females with Obesity and Food Addiction. Obesity (Silver Spring, Md.) 28, 1477–1486, doi:10.1002/oby.22870 (2020). [PubMed: 32935533]
93. Dong TS et al. Obesity is associated with a distinct brain-gut microbiome signature that connects Prevotella and Bacteroides to the brain's reward center. Gut Microbes 14, 2051999, doi:10.1080/19490976.2022.2051999 (2022). [PubMed: 35311453]
94. Dong TS et al. How Discrimination Gets Under the Skin: Biological Determinants of Discrimination Associated With Dysregulation of the Brain-Gut Microbiome System and Psychological Symptoms. Biol Psychiatry 94, 203–214, doi:10.1016/j.biopsych.2022.10.011 (2023). [PubMed: 36754687]
95. Sarnoff RP et al. A multi-omic brain gut microbiome signature differs between IBS subjects with different bowel habits. Neuropharmacology 225, 109381, doi:10.1016/j.neuropharm.2022.109381 (2023). [PubMed: 36539012]
96. Steinhardt MA, Mamerow MM, Brown SA & Jolly CA A resilience intervention in African American adults with type 2 diabetes: a pilot study of efficacy. Diabetes Educ 35, 274–284, doi:10.1177/0145721708329698 (2009). [PubMed: 19204102]
97. Bremner JD, Vermetten E & Mazure CM Development and preliminary psychometric properties of an instrument for the measurement of childhood trauma: the Early Trauma Inventory. Depress Anxiety 12, 1–12, doi:10.1002/1520-6394(2000)12:1<1::AID-DA1>3.0.CO;2-W (2000). [PubMed: 10999240]
98. Felitti VJ et al. Relationship of childhood abuse and household dysfunction to many of the leading causes of death in adults. The Adverse Childhood Experiences (ACE) Study. Am J Prev Med 14, 245–258, doi:10.1016/s0749-3797(98)00017-8 (1998). [PubMed: 9635069]
99. Rosenstiel AK & Keefe FJ The use of coping strategies in chronic low back pain patients: relationship to patient characteristics and current adjustment. Pain 17, 33–44, doi:10.1016/0304-3959(83)90125-2 (1983). [PubMed: 6226916]
100. Cohen S, Kamarck T & Mermelstein R A global measure of perceived stress. J Health Soc Behav 24, 385–396 (1983). [PubMed: 6668417]
101. Watson D, Clark LA & Tellegen A Development and validation of brief measures of positive and negative affect: the PANAS scales. J Pers Soc Psychol 54, 1063–1070, doi:10.1037//0022-3514.54.6.1063 (1988). [PubMed: 3397865]
102. Ware J Jr., Kosinski M & Keller SD A 12-Item Short-Form Health Survey: construction of scales and preliminary tests of reliability and validity. Med Care 34, 220–233, doi:10.1097/00005650-199603000-00003 (1996). [PubMed: 8628042]
103. Craig CL, Brownson RC, Cragg SE & Dunn AL Exploring the effect of the environment on physical activity: a study examining walking to work. Am J Prev Med 23, 36–43, doi:10.1016/s0749-3797(02)00472-5 (2002).
104. Craig J, Russell C, Patterson V & Wootton R User satisfaction with realtime teleneurology. J Telemed Telecare 5, 237–241, doi:10.1258/1357633991933774 (1999). [PubMed: 10829374]
105. Carver CS & White TL Behavioral inhibition, behavioral activation, and affective responses to impending reward and punishment: The BIS/BAS Scales. Journal of Personality and Social Psychology 67, 319–333 (1994).
106. Paradies Y A systematic review of empirical research on self-reported racism and health. Int J Epidemiol 35, 888–901, doi:10.1093/ije/dyl056 (2006). [PubMed: 16585055]
107. Williams DR, Yan Y, Jackson JS & Anderson NB Racial Differences in Physical and Mental Health: Socio-economic Status, Stress and Discrimination. J Health Psychol 2, 335–351, doi:10.1177/135910539700200305 (1997). [PubMed: 22013026]
108. Carver CS You want to measure coping but your protocol's too long: consider the brief COPE. Int J Behav Med 4, 92–100, doi:10.1207/s15327558ijbm0401_6 (1997). [PubMed: 16250744]

109. Kroenke K, Spitzer RL & Williams JB The PHQ-15: validity of a new measure for evaluating the severity of somatic symptoms. Psychosom Med 64, 258–266, doi:10.1097/00006842-200203000-00008 (2002). [PubMed: 11914441]
110. Carlson LE & Brown KW Validation of the Mindful Attention Awareness Scale in a cancer population. J Psychosom Res 58, 29–33, doi:10.1016/j.jpsychores.2004.04.366 (2005). [PubMed: 15771867]
111. Buysse DJ et al. Development and validation of patient-reported outcome measures for sleep disturbance and sleep-related impairments. Sleep 33, 781–792, doi:10.1093/sleep/33.6.781 (2010). [PubMed: 20550019]
112. Labus JS et al. The Visceral Sensitivity Index: development and validation of a gastrointestinal symptom-specific anxiety scale. Aliment Pharmacol Ther 20, 89–97, doi:10.1111/j.1365-2036.2004.02007.x (2004).
113. Pletikosic Toncic S & Tkalcic M A Measure of Suffering in relation to Anxiety and Quality of Life in IBS Patients: Preliminary Results. Biomed Res Int 2017, 2387681, doi:10.1155/2017/2387681 (2017). [PubMed: 28744463]
114. Roelofs J, Peters ML, McCracken L & Vlaeyen JWS The pain vigilance and awareness questionnaire (PVAQ): further psychometric evaluation in fibromyalgia and other chronic pain syndromes. Pain 101, 299–306, doi:10.1016/S0304-3959(02)00338-X (2003). [PubMed: 12583873]
115. Sullivan MJL, Bishop SR & Pivik J The Pain Catastrophizing Scale: Development and validation. Psychol Assessment 7, 524–532, doi:10.1037/1040-3590.7.4.524 (1995).
116. Osman A et al. Factor structure, reliability, and validity of the Pain Catastrophizing Scale. J Behav Med 20, 589–605, doi:10.1023/a:1025570508954 (1997). [PubMed: 9429990]
117. Costa PT & McCrae RR The Five-Factor Model of Personality and Its Relevance to Personality Disorders. J Pers Disord 6, 343–359, doi:10.1521/pedi.1992.6.4.343 (1992).
118. Costa PT & McCrae RR Multiple uses for longitudinal personality data. Eur J Personality 6, 85–102, doi:10.1002/per.2410060203 (2020).
119. Dong TS et al. Improvement in Uncontrolled Eating Behavior after Laparoscopic Sleeve Gastrectomy Is Associated with Alterations in the Brain-Gut-Microbiome Axis in Obese Women. Nutrients 12, doi:10.3390/nu12102924 (2020).
120. Osadchiy V et al. Analysis of brain networks and fecal metabolites reveals brain-gut alterations in premenopausal females with irritable bowel syndrome. Transl Psychiatry 10, 367, doi:10.1038/s41398-020-01071-2 (2020). [PubMed: 33139708]
121. Tong M, Jacobs JP, McHardy IH & Braun J Sampling of intestinal microbiota and targeted amplification of bacterial 16S rRNA genes for microbial ecologic analysis. Curr Protoc Immunol 107, 7 41 41–47 41 11, doi:10.1002/0471142735.im0741s107 (2014).
122. Callahan BJ et al. DADA2: High-resolution sample inference from Illumina amplicon data. Nat Methods 13, 581–583, doi:10.1038/nmeth.3869 (2016). [PubMed: 27214047]
123. Yilmaz P et al. The SILVA and “All-species Living Tree Project (LTP)” taxonomic frameworks. Nucleic Acids Res 42, D643–648, doi:10.1093/nar/gkt1209 (2014). [PubMed: 24293649]
124. Quast C et al. The SILVA ribosomal RNA gene database project: improved data processing and web-based tools. Nucleic Acids Res 41, D590–596, doi:10.1093/nar/gks1219 (2013). [PubMed: 23193283]
125. Glockner FO et al. 25 years of serving the community with ribosomal RNA gene reference databases and tools. J Biotechnol 261, 169–176, doi:10.1016/j.jbiotec.2017.06.1198 (2017). [PubMed: 28648396]
126. Evans AM, DeHaven CD, Barrett T, Mitchell M & Milgram E Integrated, nontargeted ultrahigh performance liquid chromatography/electrospray ionization tandem mass spectrometry platform for the identification and relative quantification of the small-molecule complement of biological systems. Anal Chem 81, 6656–6667, doi:10.1021/ac901536h (2009). [PubMed: 19624122]
127. Hatch A et al. A Robust Metatranscriptomic Technology for Population-Scale Studies of Diet, Gut Microbiome, and Human Health. Int J Genomics 2019, 1718741, doi:10.1155/2019/1718741 (2019). [PubMed: 31662956]

128. Li J et al. An integrated catalog of reference genes in the human gut microbiome. Nat Biotechnol 32, 834–841, doi:10.1038/nbt.2942 (2014). [PubMed: 24997786]
129. Chudler EH & Dong WK The role of the basal ganglia in nociception and pain. Pain 60, 3–38, doi:10.1016/0304-3959(94)00172-B (1995). [PubMed: 7715939]
130. Fischl B FreeSurfer. Neuroimage 62, 774–781, doi:10.1016/j.neuroimage.2012.01.021 (2012). [PubMed: 22248573]
131. Destrieux C, Fischl B, Dale A & Halgren E Automatic parcellation of human cortical gyri and sulci using standard anatomical nomenclature. NeuroImage 53, 1–15, doi:10.1016/j.neuroimage.2010.06.010 (2010). [PubMed: 20547229]
132. Edlow BL et al. Neuroanatomic connectivity of the human ascending arousal system critical to consciousness and its disorders. J Neuropathol Exp Neurol 71, 531–546, doi:10.1097/NEN.0b013e3182588293 (2012). [PubMed: 22592840]
133. Bhatt RR et al. Integrated multi-modal brain signatures predict sex-specific obesity status. Brain Commun 5, fcad098, doi:10.1093/braincomms/fcad098 (2023). [PubMed: 37091587]
134. Guan M et al. Improved psychosocial measures associated with physical activity may be explained by alterations in brain-gut microbiome signatures. Scientific reports 13, 10332, doi:10.1038/s41598-023-37009-z (2023). [PubMed: 37365200]
135. Labus JS et al. Sex-specific brain microstructural reorganization in irritable bowel syndrome. Pain 164, 292–304, doi:10.1097/j.pain.0000000000002699 (2023). [PubMed: 35639426]
136. Nieto-Castanon A Handbook of functional connectivity Magnetic Resonance Imaging methods in CONN. (Hilbert Press, 2020).
137. Ashburner J & Friston KJ Unified segmentation. Neuroimage 26, 839–851, doi:10.1016/j.neuroimage.2005.02.018 (2005). [PubMed: 15955494]
138. Behzadi Y, Restom K, Liau J & Liu TT A component based noise correction method (CompCor) for BOLD and perfusion based fMRI. Neuroimage 37, 90–101, doi:10.1016/j.neuroimage.2007.04.042 (2007). [PubMed: 17560126]
139. Friston KJ, Williams S, Howard R, Frackowiak RS & Turner R Movement-related effects in fMRI time-series. Magn Reson Med 35, 346–355, doi:10.1002/mrm.1910350312 (1996). [PubMed: 8699946]
140. Power JD et al. Methods to detect, characterize, and remove motion artifact in resting state fMRI. Neuroimage 84, 320–341, doi:10.1016/j.neuroimage.2013.08.048 (2014). [PubMed: 23994314]
141. Whitfield-Gabrieli S & Nieto-Castanon A Conn: a functional connectivity toolbox for correlated and anticorrelated brain networks. Brain Connect 2, 125–141, doi:10.1089/brain.2012.0073 (2012). [PubMed: 22642651]
142. Hallquist MN, Hwang K & Luna B The nuisance of nuisance regression: spectral misspecification in a common approach to resting-state fMRI preprocessing reintroduces noise and obscures functional connectivity. Neuroimage 82, 208–225, doi:10.1016/j.neuroimage.2013.05.116 (2013). [PubMed: 23747457]
143. Andersson JLR & Sotiropoulos SN An integrated approach to correction for off-resonance effects and subject movement in diffusion MR imaging. Neuroimage 125, 1063–1078, doi:10.1016/j.neuroimage.2015.10.019 (2016). [PubMed: 26481672]
144. Cook PA, B. Y, Nedjati-Gilani S, Seunarine KK, Hall MG, Parker GJ, Alexander DC. Camino: Open-Source Diffusion-MRI Reconstruction and Processing, . (2006).
145. Sarwar T, Ramamohanarao K & Zalesky A Mapping connectomes with diffusion MRI: deterministic or probabilistic tractography? Magn Reson Med 81, 1368–1384, doi:10.1002/mrm.27471 (2019). [PubMed: 30303550]
146. Singh A et al. DIABLO: an integrative approach for identifying key molecular drivers from multi-omics assays. Bioinformatics 35, 3055–3062, doi:10.1093/bioinformatics/bty1054 (2019). [PubMed: 30657866]
147. Tenenhaus A et al. Variable selection for generalized canonical correlation analysis. Biostatistics 15, 569–583, doi:10.1093/biostatistics/kxu001 (2014). [PubMed: 24550197]
148. Desikan RS et al. An automated labeling system for subdividing the human cerebral cortex on MRI scans into gyral based regions of interest. Neuroimage 31, 968–980, doi:10.1016/j.neuroimage.2006.01.021 (2006). [PubMed: 16530430]

149. Frazier JA et al. Structural brain magnetic resonance imaging of limbic and thalamic volumes in pediatric bipolar disorder. Am J Psychiatry 162, 1256–1265, doi:10.1176/appi.ajp.162.7.1256 (2005). [PubMed: 15994707]

150. Goldstein JM et al. Hypothalamic abnormalities in schizophrenia: sex effects and genetic vulnerability. Biol Psychiatry 61, 935–945, doi:10.1016/j.biopsych.2006.06.027 (2007). [PubMed: 17046727]

151. Makris N et al. Decreased volume of left and total anterior insular lobule in schizophrenia. Schizophr Res 83, 155–171, doi:10.1016/j.schres.2005.11.020 (2006). [PubMed: 16448806]

152. Backhausen LL, Herting MM, Tamnes CK & Vetter NC Best Practices in Structural Neuroimaging of Neurodevelopmental Disorders. Neuropsychol Rev 32, 400–418, doi:10.1007/s11065-021-09496-2 (2022). [PubMed: 33893904]

153. Barnes J et al. Head size, age and gender adjustment in MRI studies: a necessary nuisance? Neuroimage 53, 1244–1255, doi:10.1016/j.neuroimage.2010.06.025 (2010). [PubMed: 20600995]

154. Voevodskaya O et al. The effects of intracranial volume adjustment approaches on multiple regional MRI volumes in healthy aging and Alzheimer's disease. Front Aging Neurosci 6, 264, doi:10.3389/fnagi.2014.00264 (2014). [PubMed: 25339897]

155. Farber O & Kadmon R Assessment of alternative approaches for bioclimatic modeling with special emphasis on the Mahalanobis distance. Ecol Model 160, 115–130, doi:10.1016/s0304-3800(02)00327-7 (2003).

156. Weisberg S Applied linear regression. Fourth edition. edn, (John Wiley & Sons, Inc, 2013).

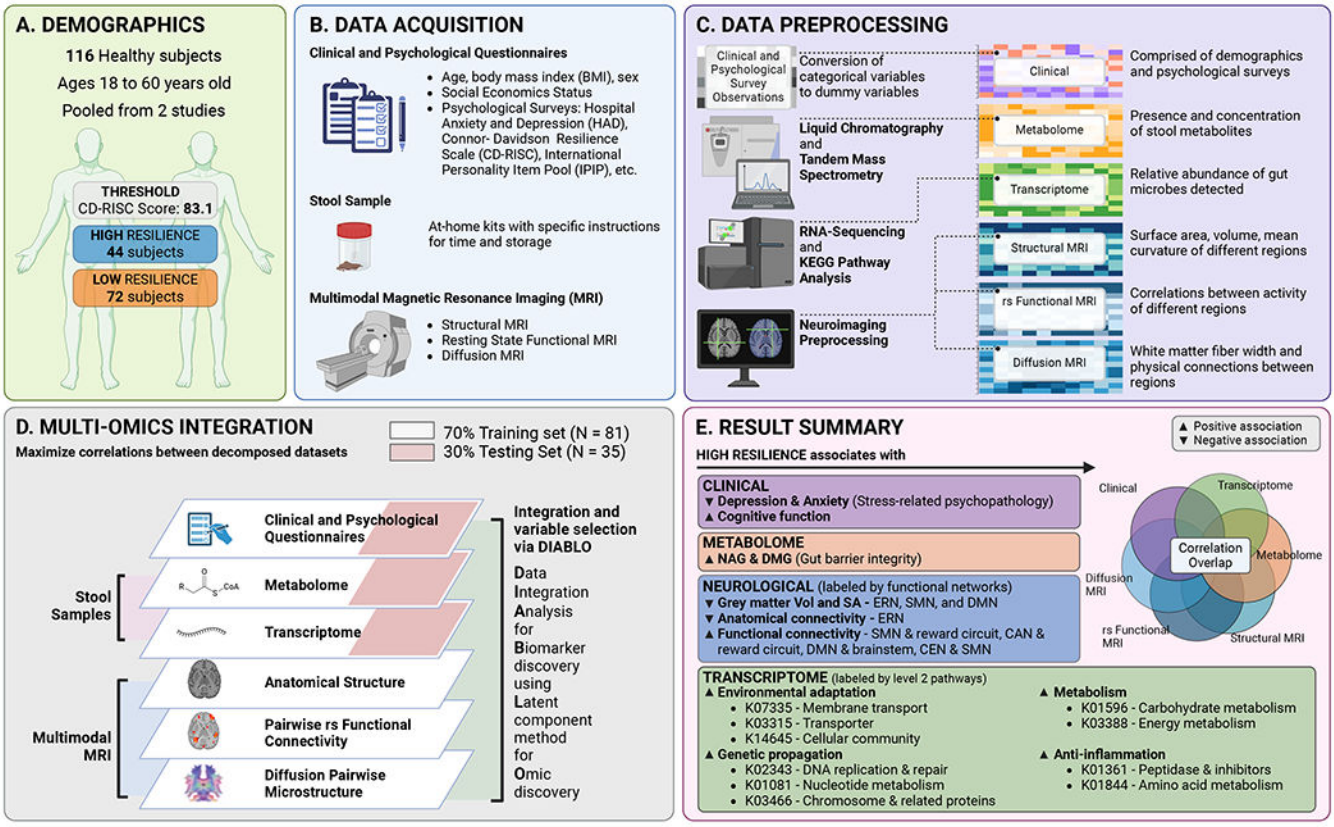

Figure 1: Graphical Summary.

A Demographics shows the CD-RISC (Connor-Davidson Resilience Scale) threshold for group label, and the sample size per group. **B** Clinical and psychological variables were collected from self-report questionnaires. Metabolites and transcriptomics data were collected from stool samples. Multimodal brain images were collected via magnetic resonance imaging. **C** Each of the six data blocks were cleaned and prepared as individual datasets. **D** Data integration for biomarker discovery using latent components as used to create signatures for high and low resilience. **E** Summary of results.

Abbreviations: BMI, body mass index; MRI, magnetic resonance imaging; RNA, Ribonucleic acid; KEGG, Kyoto Encyclopedia of Genes and Genomes; NAG, N-acetylglutamate; DMG, dimethylglycine; Vol, volume; SA, surface area; ERN, emotion regulation network; SMN, sensorimotor network; DMN, default mode network; CAN, central autonomic network; CEN, central executive network; K07335, basic membrane protein A and related proteins; K03315, Na/H antiporter; K01081, 5'-nucleotidase; K07080, uncharacterized protein; K14645, serine protease; K02343, DNA polymerase III subunit gamma/tau; K01596, phosphoenolpyruvate carboxykinase; K01361, lactocepin; K01844, beta-lysine 5,6-aminomutase alpha subunit; K03388, heterodisulfide reductase subunit A2.

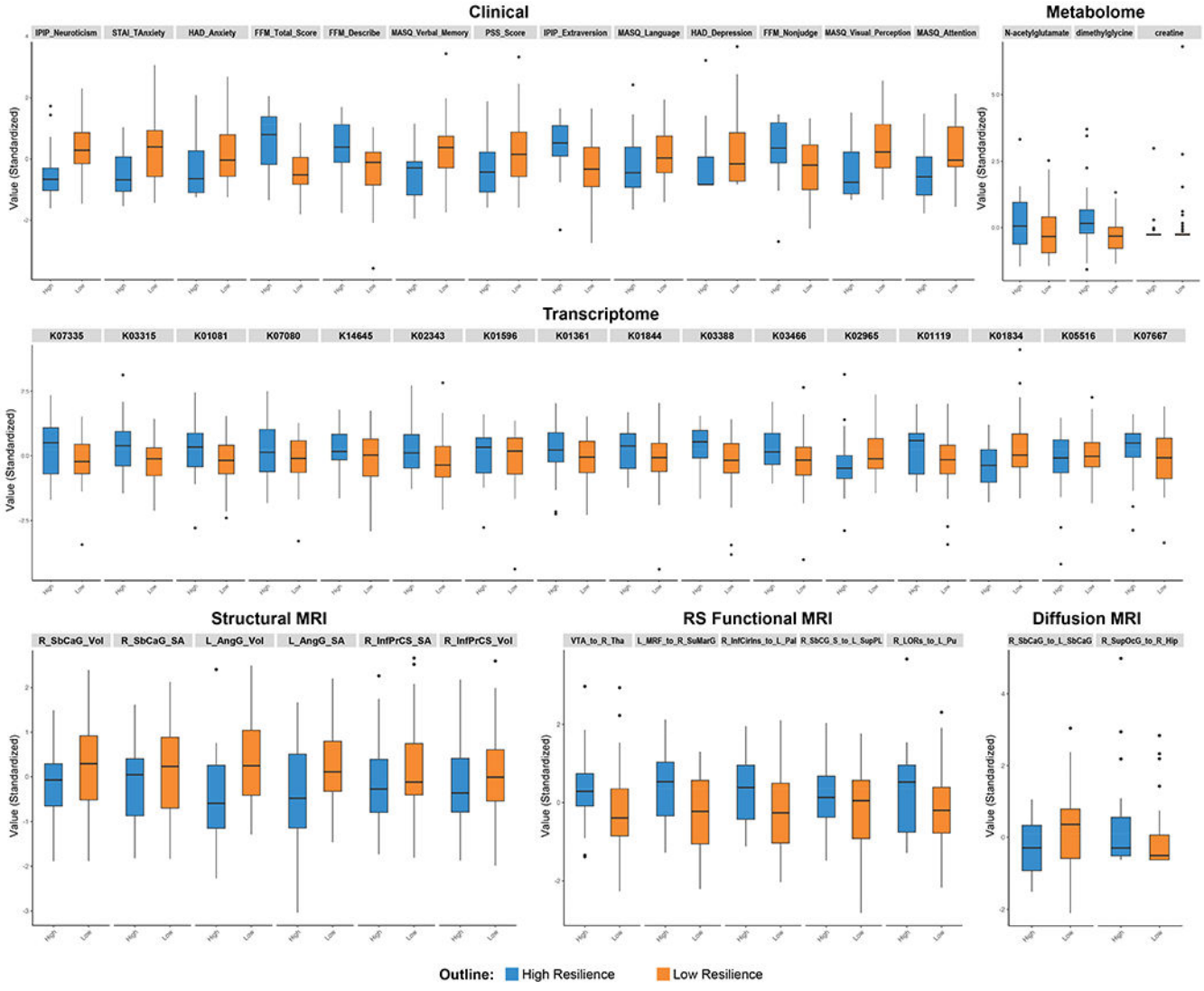

Figure 2. Boxplots of DIABLO-selected Variables of Importance.

Standardized values equate to variables of importance for each dataset between High (blue) and Low (orange) resilience. The line inside each box represents the median standardized value. Each box itself represents the interquartile range which captures 50% of standardized values. The lines extending from each box represent the ranges (extending up to the minimum and maximum) of standardized values outside of the interquartile range. Individual data points beyond the lines are considered outliers.

Abbreviations: IPIP, International Personality Item Pool; STAI, Stat-Trait Anxiety Inventory; HAD, Hospital Anxiety and Depression scale; FFM, Five Facet Mindfulness; MASQ, Multiple Ability Self-Report Questionnaire; PSS, Perceived Stress Scale; K07335, basic membrane protein A and related proteins; K03315, Na/H antiporter; K01081, 5'-nucleotidase; K07080, uncharacterized protein; K14645, serine protease; K02343, DNA polymerase III subunit gamma/tau; K01596, phosphoenolpyruvate carboxykinase; K01361, lactocepin; K01844, beta-lysine 5,6-aminomutase alpha subunit; K03388, heterodisulfide reductase subunit A2; K03466, DNA segregation ATPase FtsK/SpoIIIE; K02965, small

subunit ribosomal protein S19; K01119, 2',3'-cyclic-nucleotide 2'-phosphodiesterase / 3'-nucleotidase; K01834, 2,3-bisphosphoglycerate-dependent phosphoglycerate mutase; K05516, curved DNA-binding protein; K07667, two-component system, OmpR family, KDP operon response regulator KdpE;

R, right; L, left; SA, surface area; Vol, volume; SbCaG, Subcallosal Gyrus; AngG, Angular Gyrus; InfPrCS, Inferior part of the Precentral Sulcus; VTA, Ventral Tegmental Area; Tha, Thalamus proper; MRF, Mesencephalic Reticular Formation; SuMarG, Supramarginal Gyrus; InfCirIns, Inferior segment of the Circular Sulcus of the Insula; Pal, Pallidum; SbCG S, Subcentral Gyrus and Sulci; SupPL, Superior Parietal Lobule; LORs, Lateral Orbital Sulcus; Pu, Putamen.

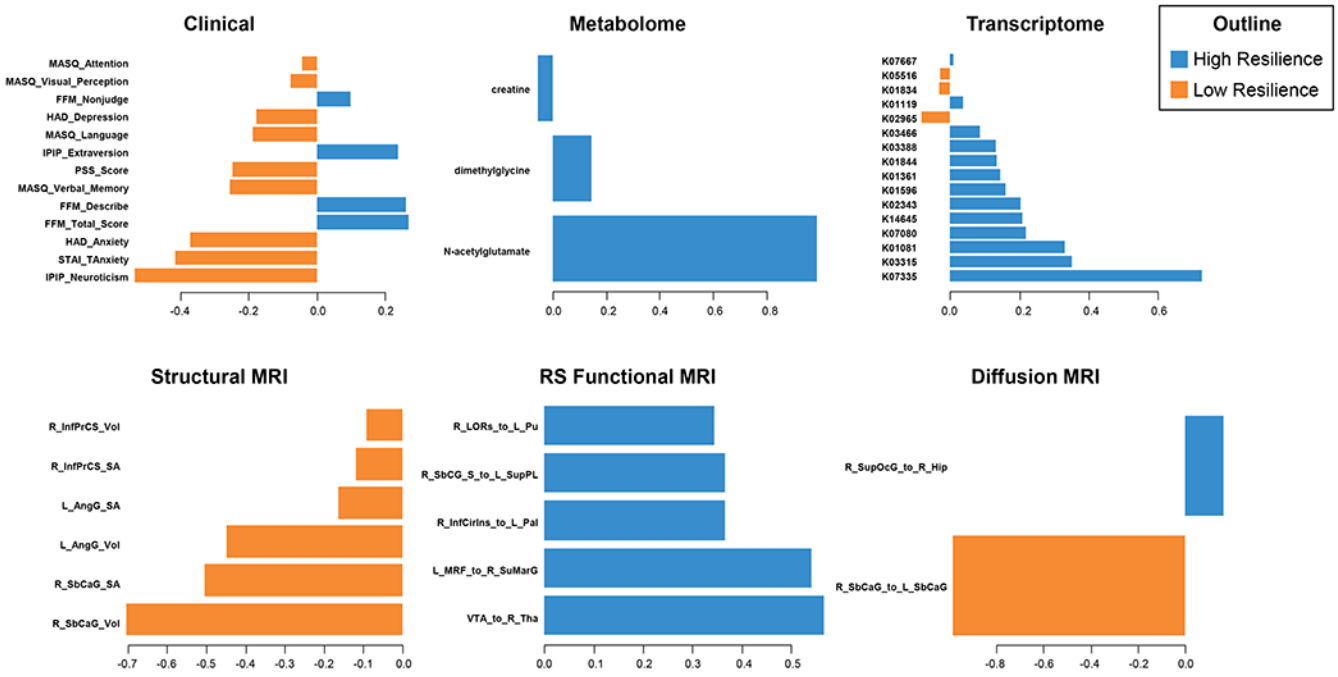

Figure 3. Loading Plots from the DIABLO-selected Variables of Importance.

Loading plots of top contributing variables selected by DIABLO separated by dataset type. Blue represents high resilience; orange represents low resilience. Magnitude of loading coefficient represents the level of contribution for prediction. Greater values represent greater contribution.

Abbreviations: MASQ, Multiple Ability Self-Report Questionnaire; FFM, Five Facet Mindfulness; HAD, Hospital Anxiety and Depression scale; IPIP, International Personality Item Pool; PSS, Perceived Stress Scale; STAI, Stat-Trait Anxiety Inventory; K07335, basic membrane protein A and related proteins; K03315, Na/H antiporter; K01081, 5'-nucleotidase; K07080, uncharacterized protein; K14645, serine protease; K02343, DNA polymerase III subunit gamma/tau; K01596, phosphoenolpyruvate carboxykinase; K01361, lactocepin; K01844, beta-lysine 5,6-aminomutase alpha subunit; K03388, heterodisulfide reductase subunit A2; K03466, DNA segregation ATPase FtsK/SpoIIIE; K02965, small subunit ribosomal protein S19; K01119, 2',3'-cyclic-nucleotide 2'-phosphodiesterase / 3'-nucleotidase; K01834, 2,3-bisphosphoglycerate-dependent phosphoglycerate mutase; K05516, curved DNA-binding protein; K07667, two-component system, OmpR family, KDP operon response regulator KdpE; MRI, magnetic resonance imaging; L, left; R, right; SbCaG, subcallosal gyrus; AngG, angular gyrus; InfPrCS, inferior part of the precentral sulcus; VTA, ventral tegmental area; Tha, thalamus; MRF, mesencephalic reticular formation; SuMarG, supramarginal gyrus; InfCirIns, inferior segment of the circular sulcus of the insula; Pal, pallidum; SupPL, superior parietal lobule; LORs, lateral orbital sulcus; Pu, putamen; SupOcG, superior occipital gyrus; Hip, hippocampus.

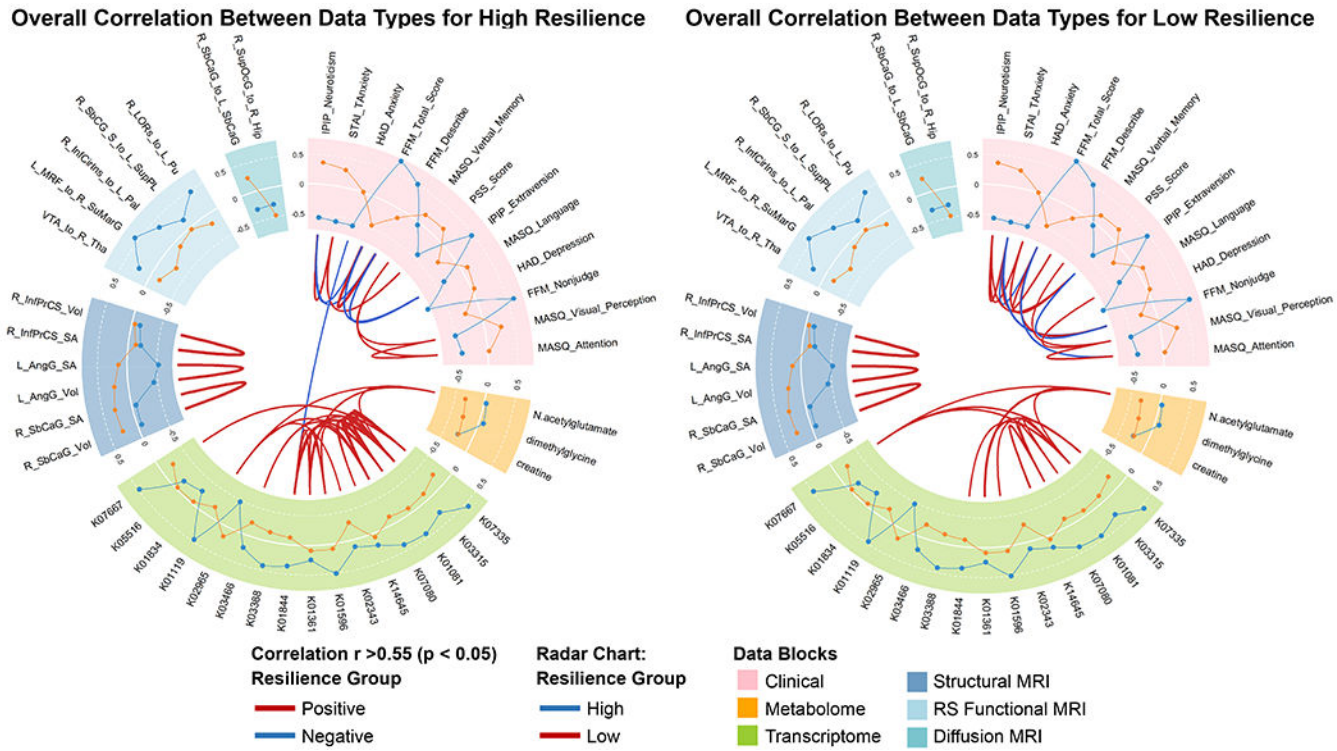

Figure 4. Connectogram Depicting the Correlations within the Variables of Importance from all the Datasets.

Spearman correlations between features across datasets are shown via the lines inside the circle (cutoff $r = 0.55$). Mean levels of each feature for each group are represented via the lines within each data block forming the circle. A higher line represents a greater mean value for that group.

Abbreviations: MRI, magnetic resonance imaging; L, left; R, right; SbCaG, subcallosal gyrus; AngG, angular gyrus; InfPrCS, inferior part of the precentral sulcus; VTA, ventral tegmental area; Tha, thalamus; MRF, mesencephalic reticular formation; SuMarG, supramarginal gyrus; InfCirIns, inferior segment of the circular sulcus of the insula; Pal, pallidum; SupPL, superior parietal lobule; LORs, lateral orbital sulcus; Pu, putamen; SupOcG, superior occipital gyrus; Hip, hippocampus; K07335, basic membrane protein A and related proteins; K03315, Na/H antiporter; K01081, 5’-nucleotidase; K07080, uncharacterized protein; K14645, serine protease; K02343, DNA polymerase III subunit gamma/tau; K01596, phosphoenolpyruvate carboxykinase; K01361, lactocepin; K01844, beta-lysine 5,6-aminomutase alpha subunit; K03388, heterodisulfide reductase subunit A2; K03466, DNA segregation ATPase FtsK/SpoIIIE; K02965, small subunit ribosomal protein S19; K01119, 2’,3’-cyclic-nucleotide 2’-phosphodiesterase / 3’-nucleotidase; K01834, 2,3-bisphosphoglycerate-dependent phosphoglycerate mutase; K05516, curved DNA-binding protein; K07667, two-component system, OmpR family, KDP operon response regulator KdpE.

Table 1.

Demographic, Clinical, Metabolome, Transcriptome, and Multimodal Brain Differences Between the High and Low Resilience Groups.

Demographic, clinical, metabolic, transcriptomic, and neurological characteristics of high and low resilience groups.

Data Block	Characteristic	N	High Resilience N = 44[1]	Low Resilience N = 72[1]	p-value[2]
Demographic/ Clinical	**Sex**	116			>0.9
	Female		27 / 44 (61%)	44 / 72 (61%)	
	Male		17 / 44 (39%)	28 / 72 (39%)	
	Age	116	34 (12)	31 (11)	0.14
	Ethnicity	116			0.89
	White		14 / 44 (32%)	18 / 72 (25%)	
	Hispanic		4 / 44 (9%)	10 / 72 (14%)	
	Asian		9 / 44 (21%)	15 / 72 (21%)	
	Black		5 / 44 (11%)	7 / 72 (10%)	
	Multiracial		12 / 44 (27%)	22 / 72 (30%)	
	BMI	116	28.1 (4.0)	27.6 (4.2)	
	Standard American Diet	116			
	0		33 / 44 (75%)	49 / 72 (68%)	
	1		11 / 44 (25%)	23 / 72 (32%)	
	Brief Resilience Score	116	25.6 (3.6)	21.4 (4.3)	**<0.001**
	CD-RISC Score	116	91 (5)	71 (9)	**<0.001**
	CD-RISC - Adaptability	116	19.00 (1.43)	15.78 (2.85)	**<0.001**
	CD-RISC - Control	116	11.05 (1.12)	8.63 (1.63)	**<0.001**
	CD-RISC - Meaning	114	6.77 (1.27)	4.62 (2.31)	**<0.001**
	CD-RISC - Persistence	116	29.8 (1.9)	23.8 (3.9)	**<0.001**
	CD-RISC - Emotional Cognitive Control	116	24.4 (2.5)	18.2 (3.6)	**<0.001**
	FFM - Describe	91	32 (6)	28 (6)	**0.004**
	FFM - Nonjudge	89	32 (7)	28 (7)	**0.001**
	FFM - Total Score	87	149 (20)	132 (15)	**<0.001**
	HADS - Anxiety	116	3 (3)	5 (3)	**0.013**
	HADS - Depression	116	1 (2)	2 (2)	**0.003**
	IPIP - Extraversion	113	38 (6)	33 (7)	**<0.001**
	IPIP - Neuroticism	113	17 (5)	23 (6)	**<0.001**
	MASQ - Attention	102	14 (4)	17 (4)	**<0.001**
	MASQ - Language	102	14 (4)	15 (4)	0.081
	MASQ - Verbal Memory	101	15.4 (3.9)	18.5 (4.6)	**<0.001**
	MASQ - Visual Perception	102	9.5 (3.2)	11.9 (3.9)	**0.001**
	PSS Score	116	10 (5)	13 (7)	**0.002**
	STAI - Anxiety	116	43 (7)	50 (10)	**<0.001**
	N-acetylglutamate	104	1.37 (0.72)	1.07 (0.57)	**0.033**

Data Block	Characteristic	N	High Resilience N = 44[1]	Low Resilience N = 72[1]	p-value[2]
Metabolome	**dimethylglycine**	98	1.28 (0.67)	1.08 (0.61)	0.13
	creatine	104	5 (16)	9 (31)	0.3
	K07335	116	1.95 (0.57)	1.68 (0.47)	**0.012**
Transcriptome	**K03315**	116	0.64 (0.79)	0.17 (0.68)	**0.002**
	K01081	116	0.51 (0.53)	0.23 (0.50)	**0.007**
	K07080	116	0.12 (0.94)	−0.33 (1.07)	**0.018**
	K14645	116	−1.21 (0.95)	−1.82 (1.43)	**0.007**
	K02343	116	0.42 (0.42)	0.27 (0.44)	0.064
	K01596	116	−0.21 (1.03)	−0.53 (1.16)	0.12
	K01361	116	−0.86 (1.92)	−1.50 (1.76)	0.080
	K01844	116	−0.47 (0.91)	−0.93 (1.20)	**0.022**
	K03388	116	−0.79 (0.78)	−1.35 (1.09)	**0.002**
	K03466	116	0.17 (0.30)	0.01 (0.36)	**0.013**
	K02965	116	1.91 (0.43)	2.18 (0.41)	**0.002**
	K01119	116	0.07 (0.56)	−0.25 (0.58)	**0.004**
	K01834	116	1.68 (0.24)	1.89 (0.39)	**<0.001**
	K05516	116	0.41 (1.50)	0.93 (1.20)	0.053
	K07667	116	−0.39 (0.69)	−0.67 (0.76)	**0.045**
	R SbCaG Volume	116	−0.32 (0.80)	0.06 (1.08)	**0.030**
Structural MRI	**R SbCaG Surface Area**	116	−0.16 (1.01)	0.03 (1.01)	**0.3**
	L AngG Volume	116	−0.46 (0.85)	0.23 (0.93)	**<0.001**
	L AngG Surface Area	116	−0.46 (1.01)	0.20 (0.94)	**<0.001**
	R InfPrCS Surface Area	116	−0.02 (0.93)	0.11 (0.98)	0.5
	R InfPrCS Volume	116	0.00 (0.92)	0.09 (1.04)	0.6
	VTA to R Tha	116	0.12 (0.14)	0.06 (0.13)	**0.029**
rs Functional MRI	**L MRF to R SuMarG**	116	0.07 (0.11)	−0.01 (0.12)	**<0.001**
	R InfCirIns to L Pal	116	0.10 (0.15)	0.04 (0.15)	**0.034**
	R SbCG S to L SupPL	116	−0.05 (0.16)	−0.08 (0.17)	0.2
	R LORs to L Pu	116	0.06 (0.15)	0.00 (0.15)	**0.046**
	R SbCaG to L SbCaG	116	0.0006 (0.0002)	0.0007 (0.0003)	0.056
Diffusion MRI	**R SupOcG to R Hip**	116	0.0001 (0.0001)	0.0000 (0.0001)	0.2
	R SupOcG to R Hip	116	0.0001 (0.0001)	0.0000 (0.0001)	0.2

Abbreviations: BMI, body mass index; CD-RISC, Connor-Davidson Resilience Scale; MASQ, Multiple Ability Self-Report Questionnaire; FFM, Five Facet Mindfulness; HADS, Hospital Anxiety and Depression scale; IPIP, International Personality Item Pool; PSS, Perceived Stress Scale; STAI, Stat-Trait Anxiety Inventory; K07335, basic membrane protein A and related proteins; K03315, Na/H antiporter; K01081, 5'-nucleotidase; K07080, uncharacterized protein; K14645, serine protease; K02343, DNA polymerase III subunit gamma/tau; K01596, phosphoenolpyruvate carboxykinase; K01361, lactocepin; K01844, beta-lysine 5,6-aminomutase alpha subunit; K03388, heterodisulfide reductase subunit A2; K03466, DNA segregation ATPase FtsK/SpoIIIE; K02965, small subunit ribosomal protein S19; K01119, 2',3'-cyclic-nucleotide 2'-phosphodiesterase / 3'-nucleotidase; K01834, 2,3-bisphosphoglycerate-dependent phosphoglycerate mutase; K05516, curved DNA-binding protein; K07667, two-component system, OmpR family, KDP operon response regulator KdpE. R, right; L, left; SA, surface area; Vol, volume; SbCaG, Subcallosal Gyrus; AngG, Angular Gyrus; InfPrCS, Inferior part of the Precentral Sulcus; VTA, Ventral Tegmental Area; Tha, Thalamus proper; MRF, Mesencephalic Reticular Formation; SuMarG, Supramarginal Gyrus; InfCirIns, Inferior segment of the Circular Sulcus of the Insula; Pal, Pallidum; SbCG S, Subcentral Gyrus and Sulci; SupPL, Superior Parietal Lobule; LORs, Lateral Orbital Sulcus; Pu, Putamen; SupOcG, Superior Occipital Gyrus; Hip, Hippocampus.

[1] n / N (%); Mean (standard deviation)

[2]Pearson's Chi-squared test; Welch Two Sample t-test

Table 2.

Correlations of Participant Characteristics and Omics Variables Selected by the DIABLO Model with CD-RISC Sub-scales.

Spearman's correlations of participant demographics and DIABLO selected variables with Total CD-RISC score, and Adaptability, Control, Meaning, Persistence, and Emotional Cognitive control sub-scales. Adaptability represents ability to bounce back and relates to the positive acceptance of change and secure relationships. Control meaning refers to individual's perception of control over their life circumstances. Higher scores represent having a sense of control and a tendency to view challenges as manageable and belief that one has some influence over outcomes which enhance resilience by promoting problem-solving and adaptive coping strategies. Meaning relates to spiritual influences. Persistence refers to a sense of self-efficacy and reflects a sense of personal competence and high standards. Emotional Cognitive control scores control under pressure, trust in one's instincts and tolerance of negative affects. P-value < 0.05 (Significant)

Data Block	Variable	Total Score		Adaptability		Control		Meaning		Persistence		Emotional Cognitive Control	
		R	p	R	p	R	p	R	p	R	p	R	p
Demographics	Sex	−0.0424	0.6511	−0.0618	0.5097	0.0896	0.3387	0.1287	0.1724	−0.0851	0.3636	−0.1027	0.2728
	Age	0.1281	0.1704	−0.0312	0.7393	0.2072	**0.0256**	0.1756	0.0616	0.0871	0.3524	0.1342	0.1509
	BMI	0.0808	0.3883	0.0428	0.6486	0.0586	0.5321	0.0676	0.4750	0.0562	0.5493	0.0932	0.3199
	Standard American Diet	0.0611	0.5148	−0.0993	0.2891	0.1172	0.2101	0.1152	0.2223	0.0607	0.5174	0.0722	0.4413
Clinical	Brief Resilience Score	0.6715	**0.0000**	0.6152	**0.0000**	0.5149	**0.0000**	0.1736	0.0647	0.6143	**0.0000**	0.6138	**0.0000**
	FFM - Describe	0.3389	**0.0010**	0.3059	**0.0032**	0.4181	**0.0000**	0.2044	0.0547	0.2681	**0.0102**	0.2371	**0.0237**
	FFM - Nonjudge	0.4687	**0.0000**	0.3911	**0.0002**	0.4519	**0.0000**	0.1582	0.1434	0.4769	**0.0000**	0.3518	**0.0007**
	FFM - Total Score	0.5345	**0.0000**	0.4454	**0.0000**	0.5229	**0.0000**	0.1938	0.0755	0.4819	**0.0000**	0.4531	**0.0000**
	HADS - Anxiety	−0.4190	**0.0000**	−0.2951	**0.0013**	−0.4311	**0.0000**	−0.0876	0.3540	−0.4274	**0.0000**	−0.3599	**0.0001**
	HADS - Depression	−0.5104	**0.0000**	−0.5093	**0.0000**	−0.5065	**0.0000**	−0.1163	0.2177	−0.4418	**0.0000**	−0.4217	**0.0000**
	IPIP - Extraversion	0.4690	**0.0000**	0.3881	**0.0000**	0.4782	**0.0000**	0.2304	**0.0150**	0.4321	**0.0000**	0.3522	**0.0001**
	IPIP - Neuroticism	−0.5935	**0.0000**	−0.5298	**0.0000**	−0.4870	**0.0000**	−0.0645	0.5013	−0.6341	**0.0000**	−0.4980	**0.0000**
	MASQ - Attention	−0.5460	**0.0000**	−0.3877	**0.0001**	−0.4351	**0.0000**	−0.1388	0.1686	−0.5352	**0.0000**	−0.5286	**0.0000**
	MASQ - Language	−0.3905	**0.0000**	−0.4462	**0.0000**	−0.3115	**0.0014**	0.0530	0.6004	−0.4040	**0.0000**	−0.3333	**0.0006**
	MASQ – Verbal Memory	−0.4836	**0.0000**	−0.3035	**0.0020**	−0.4830	**0.0000**	−0.1775	0.0788	−0.4305	**0.0000**	−0.4660	**0.0000**
	MASQ - Visual Perception	−0.3730	**0.0001**	−0.3467	**0.0004**	−0.3190	**0.0011**	−0.0225	0.8238	−0.3515	**0.0003**	−0.3511	**0.0003**
	PSS - Score	−0.5098	**0.0000**	−0.4116	**0.0000**	−0.5298	**0.0000**	−0.1402	0.1368	−0.4940	**0.0000**	−0.4109	**0.0000**
	STAI - Anxiety	−0.6287	**0.0000**	−0.6153	**0.0000**	−0.5603	**0.0000**	−0.1436	0.1276	−0.5816	**0.0000**	−0.5170	**0.0000**

Data Block	Variable	Total Score		Adaptability		Control		Meaning		Persistence		Emotional Cognitive Control	
		R	p	R	p	R	p	R	p	R	p	R	p
Metabolome	N-acetylglutamate	0.1623	0.0997	0.0933	0.3464	0.2240	**0.0223**	0.0634	0.5267	0.1032	0.2972	0.1710	0.0827
	Dimethylglycine	−0.0139	0.8917	−0.0863	0.3983	0.0537	0.5996	0.0552	0.5932	−0.0376	0.7134	−0.0060	0.9533
	Creatine	−0.2416	**0.0135**	−0.1297	0.1894	−0.2656	**0.0064**	−0.1605	0.1071	−0.2333	**0.0172**	−0.1782	0.0703
Transcriptome	K07335	0.2408	**0.0092**	0.1396	0.1351	0.2866	**0.0018**	0.0766	0.4182	0.2982	**0.0011**	0.1494	0.1095
	K03315	0.2063	**0.0263**	0.1328	0.1553	0.1873	**0.0441**	0.0529	0.5761	0.2226	**0.0163**	0.1829	0.0494
	K01081	0.1358	0.1461	0.0572	0.5420	0.1898	**0.0412**	0.1293	0.1705	0.1318	0.1584	0.0771	0.4105
	K07080	0.1183	0.2058	0.1346	0.1496	0.1241	0.1845	−0.0048	0.9594	0.1386	0.1380	0.0686	0.4643
	K14645	0.1442	0.1224	0.0720	0.4426	0.1819	0.0507	0.1832	0.0510	0.1119	0.2319	0.0942	0.3146
	K02343	0.1749	0.0604	0.0996	0.2872	0.1842	**0.0478**	0.0163	0.8635	0.2127	**0.0219**	0.1427	0.1265
	K01596	0.2705	**0.0033**	0.1767	0.0578	0.2848	**0.0019**	0.1656	0.0783	0.2645	**0.0041**	0.1973	**0.0338**
	K01361	0.1916	**0.0394**	0.0697	0.4570	0.2007	0.0307	0.1531	0.1039	0.1887	**0.0424**	0.1607	0.0849
	K01844	0.2080	**0.0251**	0.0775	0.4083	0.2676	**0.0037**	0.1762	0.0607	0.2084	**0.0248**	0.1427	0.1264
	K03388	0.2522	**0.0063**	0.2002	**0.0312**	0.2725	**0.0031**	0.0502	0.5962	0.2720	**0.0031**	0.1832	**0.0490**
	K03466	0.1844	**0.0475**	0.1019	0.2764	0.2238	**0.0158**	0.0105	0.9119	0.2408	**0.0092**	0.1240	0.1848
	K02965	−0.1880	**0.0433**	−0.1876	**0.0438**	−0.1580	0.0902	−0.0887	0.3482	−0.1604	0.0854	−0.1528	0.1015
	K01119	0.1712	0.0662	0.0963	0.3039	0.1672	0.0729	0.2378	**0.0108**	0.1086	0.2457	0.1326	0.1558
	K01834	−0.2441	**0.0083**	−0.1453	0.1195	−0.2214	**0.0169**	−0.2148	**0.0217**	−0.2492	**0.0070**	−0.1580	0.0902
	K05516	−0.1948	**0.0361**	−0.1940	**0.0369**	−0.1877	**0.0436**	−0.0055	0.9534	−0.1875	**0.0438**	−0.1703	0.0677
	K07667	0.0165	0.8602	−0.0300	0.7490	0.1004	0.2833	0.0553	0.5588	0.0315	0.7371	−0.0306	0.7440
Structural MRI	R SbCaG Vol	−0.2085	0.0247	−0.2589	**0.0050**	−0.2150	0.0204	−0.0037	0.9691	−0.1790	0.0545	−0.1582	0.0900
	R SbCaG SA	−0.1138	0.2240	−0.1785	0.0552	−0.1488	0.1108	0.0305	0.7473	−0.0939	0.3158	−0.0712	0.4474
	L AngG Vol	−0.2401	**0.0094**	−0.2194	**0.0180**	−0.2163	**0.0197**	0.0302	0.7496	−0.2220	**0.0166**	−0.2553	**0.0057**
	L AngG SA	−0.2190	**0.0182**	−0.2461	**0.0078**	−0.1763	0.0583	0.0218	0.8182	−0.1922	**0.0388**	−0.2162	**0.0198**
	R InfPrCS SA	−0.1191	0.2028	−0.1170	0.2108	−0.1306	0.1625	−0.1423	0.1311	−0.0694	0.4592	−0.0711	0.4483
	R InfPrCS Vol	−0.0930	0.3206	−0.0736	0.4324	−0.0992	0.2896	−0.1036	0.2725	−0.0508	0.5885	−0.0775	0.4083
rs Functional MRI	VTA to R Tha	0.1827	**0.0496**	0.1555	0.0956	0.1567	0.0930	0.1320	0.1615	0.1529	0.1013	0.1401	0.1335
	L MRF to R SuMarG	0.2659	**0.0039**	0.1848	**0.0470**	0.2537	**0.0060**	0.0651	0.4915	0.2836	**0.0020**	0.2231	**0.0161**
	R InfCirIns to L Pal	0.1801	0.0531	0.1135	0.2252	0.1842	**0.0478**	0.1468	0.1190	0.1500	0.1079	0.1467	0.1162
	R SbCG S to L SupPL	0.1432	0.1251	0.1144	0.2216	0.1889	**0.0423**	0.1305	0.1662	0.1350	0.1485	0.0576	0.5388
	R LORs to L Pu	0.1956	**0.0354**	0.1127	0.2284	0.1751	0.0601	0.1891	**0.0439**	0.2058	**0.0266**	0.1163	0.2137
Diffusion MRI	R SbCaG to L SbCaG	−0.2406	**0.0093**	−0.1567	0.0930	−0.3306	**0.0003**	−0.1463	0.1204	−0.2416	**0.0090**	−0.1350	0.1485
	R SupOcG to R Hip	0.1912	**0.0398**	0.1712	0.0662	0.1685	0.0706	0.0663	0.4835	0.1332	0.1542	0.2027	**0.0291**

Abbreviations: BMI, body mass index; CD-RISC, Connor-Davidson Resilience Scale; FFM, Five Facet Mindfulness; HADS, Hospital Anxiety and Depression Scale; IPIP, International Personality Pool; MASQ, Multiple Ability Self-Report Questionnaire; PSS, Perceived Stress Scale; STAI, State-Trait Anxiety Inventory; K07335, basic membrane protein A and related proteins; K03315, Na/H antiporter; K01081, 5'-nucleotidase;

K07080, uncharacterized protein; K14645, serine protease; K02343, DNA polymerase III subunit gamma/tau; K01596, phosphoenolpyruvate carboxykinase; K01361, lactocepin; K01844, beta-lysine 5,6-aminomutase alpha subunit; K03388, heterodisulfide reductase subunit A2; K03466, DNA segregation ATPase FtsK/SpoIIIE; K02965, small subunit ribosomal protein S19; K01119, 2',3'-cyclic-nucleotide 2'-phosphodiesterase / 3'-nucleotidase; K01834, 2,3-bisphosphoglycerate-dependent phosphoglycerate mutase; K05516, curved DNA-binding protein; K07667, two-component system, OmpR family, KDP operon response regulator KdpE; MRI, magnetic resonance imaging; L, left; R, right; SbCaG, subcallosal gyrus; AngG, angular gyrus; InfPrCS, inferior part of the precentral sulcus; VTA, ventral tegmental area; Tha, thalamus; MRF, mesencephalic reticular formation; SuMarG, supramarginal gyrus; InfCirIns, inferior segment of the circular sulcus of the insula; Pal, pallidum; SupPL, superior parietal lobule; LORs, lateral orbital sulcus; Pu, putamen; SupOcG, superior occipital gyrus; Hip, hippocampus